J. Dairy Sci. 108:13938–13957
https://doi.org/10.3168/jds.2025-26916

Prepartal liver glutathione and its association with lactation performance, metabolism, and health outcomes in transition dairy cows

A. F. S. Lima,[1] M. H. De Oliveira,[1] G. G. Begalli,[1] R. C. B. Grazziotin,[1] J. Halfen,[1] E. Trevisi,[2] and J. S. Osorio[1]*
[1]School of Animal Science, Virginia Tech, Blacksburg, VA 24061
[2]Department of Animal Sciences, Food and Nutrition (DIANA), Faculty of Agriculture, Food and Environmental Sciences, Università Cattolica del Sacro Cuore, 29122 Piacenza, Italy

ABSTRACT

Our objective was to determine the association of prepartal liver glutathione (GSH) concentration with lactation performance parameters, metabolism and inflammation, and gene expression in transition dairy cows. Sixty Holstein dairy cows were enrolled at −21 ± 3.3 d relative to calving and remained on trial until 30 DIM. All cows received the same close-up diet from −21 DIM until calving (1.67 Mcal/DM and 13.5% CP) and lactation diet from calving until 30 DIM (1.80 Mcal/DM and 17.7% CP). A liver biopsy was performed in all cows at −8 d (±3.2 d) relative to calving, and total GSH was measured using a commercial colorimetric kit. This metric was used to retrospectively classify cows by GSH as high (HGSH; n = 15), medium-high (MHGSH; n = 15), medium-low (MLGSH; n = 15), and low (LGSH; n = 15). Liver samples were collected at −8, 7, and 21 DIM, and blood samples at −21, −10, 2, 7, 14, and 21 DIM to evaluate oxidative stress, metabolism, inflammation, and liver function biomarkers. Statistical analysis was performed using the MIXED procedure of SAS (SAS Institute Inc., Cary, NC) with the preplanned contrast to test a linear effect with increasing levels of GSH. A linear increase in prepartal energy balance (EB; from −1.55 to 1.11 Mcal/d) and postpartal BCS (from 3.00 to 3.16) was observed as prepartal liver GSH increased from LGSH to HGSH groups, suggesting an association between prepartal liver GSH and energy metabolism around parturition. This effect was also associated with a trend for a linear increase in prepartal DMI as prepartal liver GSH increased across groups. We observed a linear increase in ECM (from 50.2 to 54.7 kg/d) and milk protein yield (from 1.33 to 1.46 kg/d) as prepartal liver GSH levels increased. Neither reactive oxygen metabolites nor antioxidant capacity measured via ferric reducing antioxidant power were altered according to prepartal liver GSH. However, there was a linear increase in the total thiol groups of plasma as prepartal liver GSH increased, suggesting some level of antioxidant protection. A linear increase in total (from 0.83 to 1.74 nmol/mg), reduced (from 0.66 to 1.37 nmol/mg), and oxidized forms of GSH (from 0.07 to 0.17 nmol/mg) was observed in the liver as prepartal liver GSH levels increased. The hepatic activity of gamma-glutamyl-transferase at −8 DIM was greater in MHGSH cows compared with LGSH and HGSH. At −8 DIM, a linear upregulation of genes related to GSH metabolism, including *GCLC*, *GGCT*, and *GSR*, was observed as prepartal liver GSH increased, suggesting that transcriptional regulation may contribute to the GSH phenotype observed in this study. These results emphasize the importance of maintaining adequate hepatic GSH reserves before calving to support metabolic adaptation and lactation performance. Future research should explore the direct effect of GSH on lactation performance and oxidative stress protection, as well as nutritional and management factors to enhance hepatic GSH synthesis before calving.
Key words: transition cow, glutathione, liver metabolism

INTRODUCTION

The transition period is a well-known critical stage in the life cycle of dairy cows, substantially influencing their overall health and lactation performance. During this period, cows experience an orchestrated metabolic adaptation leading to negative energy and protein balance, which enables their bodies to support their physiological state (Baumgard et al., 2017; Trevisi and Minuti, 2018). One of the main challenges faced by these animals is oxidative stress, which arises from an imbalance between the increase of oxidative factors, such as reactive oxygen metabolites (**ROM**), and depleted antioxidants (Sordillo and Aitken, 2009). The oxidative stress derived from excessive fatty acid oxidation and immune cell activation (i.e., phagocytosis and oxidative

Received May 10, 2025.
Accepted August 26, 2025.
*Corresponding author: osorio@vt.edu

The list of standard abbreviations for JDS is available at adsa.org/jds-abbreviations-25. Nonstandard abbreviations are available in the Notes.

burst), along with metabolic dysregulation, can increase the susceptibility to diseases during the transition period. Therefore, nutritional and management strategies that enhance antioxidant capacity during the transition period are important to improve health outcomes during this time (Abuelo et al., 2015).

A substantial number of the endogenous antioxidant defense mechanisms that help regulate reactive oxygen species production in dairy cattle come from dietary sources, including vitamins, AA, and minerals (Sordillo, 2016). For instance, Met is an upstream precursor of glutathione (**GSH**) through the transsulfuration pathway (Coleman et al., 2021). Feeding rumen-protected methionine (**RPM**) during the transition period has been consistently reported to increase GSH concentration in the liver of dairy cows (Osorio et al., 2014b; Zhou et al., 2016; Batistel et al., 2018). In addition to antioxidant properties, GSH has been regarded as a reservoir of AA when stored in the liver due to its tripeptide structure, including Glu, Cys, and Gly (Lu, 2009). This particular effect in dairy cows was reviewed by Baumrucker (1985), highlighting the importance of glutathione in supplying a significant amount of Glu, Cys, and Gly to the mammary gland. In addition, using in vitro experiments, Baumrucker (1985) pointed out that the key roles of gamma-glutamyl transferase (**GGT**) along with AA transporters in the mammary gland were to break down GSH and take up constituent GSH-AA during lactation. This enhanced uptake of AA via GSH has been correlated with increased milk yield and milk protein synthesis in dairy cattle (Atroshi and Sandholm, 1982; Osorio et al., 2014b; Zhou et al., 2016).

The synthesis of GSH involves 2 ATP-dependent steps: the initial step is catalyzed by L-glutamate L-cysteine γ-ligase (**GCL**), producing γ-glutamyl-cysteine, and the second step is catalyzed by GSH synthetase (**GSS**), which adds a glycine molecule to γ-glutamyl-cysteine to form GSH (Lu, 2013). The activity of GCL has been reported as the rate-limiting step in GSH biosynthesis (Dalton et al., 2004). This was supported by findings that overexpression of *GCLC* and not *GSS* is associated with increased GSH levels (Lu, 2013). Increasing the supply of GSH precursors such as Met could lead to activation or upregulation of GSH-synthesis-related genes. However, this effect has been mainly reported in vitro (Zhou et al., 2018) but not in vivo (Osorio et al., 2014a; Zhou et al., 2017).

Despite the well-documented importance of GSH peroxidase (**GPx**) in cellular redox balance and protection against oxidative damage, the specific mechanisms by which liver GSH influences homeorhetic status in dairy cows remain underexplored, particularly in the peripartum period. Our hypothesis was that cows with higher prepartal liver GSH will have access to a greater reservoir of readily available antioxidants and AA in the form of GSH after calving, when dairy cows have a high requirement for these nutrients. The objective of this study was to determine potential mechanisms regulating the synthesis and degradation of prepartal liver GSH to better understand its prepartal accumulation in transition dairy cows and evaluate the association of prepartal liver GSH concentration with lactation performance, metabolism, inflammation, and gene expression during early lactation.

MATERIALS AND METHODS

All procedures were conducted under protocols approved by the Virginia Tech Institutional Animal Care and Use Committee (protocol no. 22-071). Eighty-seven multiparous Holstein dairy cows from Virginia Tech Dairy Science Complex (Blacksburg, VA) were enrolled at −21 ± 3.3 d relative to calving and remained on trial until 30 DIM. Twenty-seven cows were removed from the experiment for the following reasons: calved before the −8 d liver biopsy (n = 7); calved within 3 d after the −8 d liver biopsy (n = 6); tissue not collected during −8 d liver biopsy (n = 4); calved 12 d after the due date (n = 1); health-related problems such as metritis (n = 1), hypocalcemia (n = 2), displaced abomasum (n = 1), and leg injury (n = 1); calved twins (n = 1); transponder malfunction leading to missing milk production data (n = 1); and failure to learn to use the Calan gate feeding system (n = 2). A liver biopsy was targeted for all cows at −10 d relative to expected calving; however, actual biopsy was performed at −8 ± 3.2 d relative to calving. Actual biopsy days relative to calving for high (**HGSH**), medium-high (**MHGSH**), medium-low (**MLGSH**), and low GSH (**LGSH**) groups were −10 ± 3.3, −7 ± 3.0, −7 ± 2.8, and −7 ± 2.5, respectively. This prepartal liver biopsy was used to measure total GSH. This metric was used to perform retrospective analysis using the PROC UNIVARIATE procedure in SAS (SAS/STAT version 9.4, SAS Institute Inc., Cary, NC) and assign cows into quartile groups (n = 15 per group) as follows: HGSH, 2.37 ± 0.07 nmol/mg; MHGSH, 1.60 ± 0.07 nmol/mg; MLGSH, 1.14 ± 0.07 nmol/mg; and LGSH, 0.48 ± 0.07 nmol/mg.

A 2-tailed sample size was calculated using the POWER procedure of SAS (SAS/STAT version 9.4, SAS Institute Inc., Cary, NC). We evaluated the power of the study to detect differences in liver GSH, the main variable in question, and the classification variable. We used variance data on prepartal liver GSH levels from a previous trial (Osorio et al., 2014b) and found that 68 cows (17/treatment) would provide 80% power to detect a 0.72-m*M* difference in liver GSH. To account for potential attrition during the experiment, additional cows were enrolled to result in 87 total cows. Never-

theless, the experiment was planned to use orthogonal contrasts to test linear and quadratic effects on incremental levels of liver GSH.

Animal Management

Cows were enrolled in the experiment from early July 2022 to early March 2023. All cows received the same close-up diet from −21 DIM ± 3 until calving (1.67 Mcal/kg of DM and 13.5% CP) and a lactation diet from calving until 30 DIM (1.80 Mcal/kg of DM and 17.7% CP; Table 1). Diets were formulated using the Cornell Net Carbohydrate and Protein System model contained within the Agricultural Modeling and Training Systems CattlePro diet-balancing software (version 4.16.1, AMTS LLC, Groton, NY) to meet the requirements of the average cow in the group. After completion of the trial, diet formulation was evaluated with the NASEM (2021) model using the chemical analysis of feed ingredients (Table 1). Cows were fed once a day (~0800 h). Close-up cows were housed in a compost-bedded pack barn with an individual Calan gate feeding system (American Calan, Northwood, NH). On d 3 postpartum, cows were moved to a sand-bedded freestall barn with an individual Calan gate feeding system and milked 2 times daily at ~0100 and 1200 h. At 30 DIM, cows returned to the farm herd.

Body weight was measured weekly during the close-up period before the morning feeding for each cow. During lactation, BW was measured daily after milking using an automatic scale. Body condition score (scale of 1 = thin to 5 = obese, with quarter-point increments) was recorded weekly by 2 individuals, and the average score was used for statistical analysis.

Individual health checks were conducted at 1, 3, 5, 7, 9, and 11 d relative to parturition. Rectal temperature (GLA M900 Thermometer, GLA Agricultural Electronics, CA) and ketone concentration in blood (Precision Xtra β-ketone, Abbott Diabetes Care) were measured. Cows with a higher ketone body level (≥2.1 mmol/dL) were treated with propylene glycol for 3 d. If cows produced less than 5 L of colostrum, they received a calcium bolus as part of the farm's management practice to prevent hypocalcemia. Cows experiencing any problems after calving (such as retained placenta, hypocalcemia, and metritis, among other factors) were evaluated by the veterinarian and treated by the farm management.

Table 1. Ingredients diet composition during the close-up (−21 d to calving) and early lactation (calving to 30 DMI)

	Diet	
Component	Close-up	Fresh lactation
Ingredient (% DM)		
Corn silage	51.56	40.39
Alfalfa hay	—	5.77
Grass hay	19.83	—
Corn grain, finely ground	11.11	18.65
Soybean meal	15.07	5.03
Soy plus	—	8.69
Blood meal	—	1.83
Soybean hulls ground	—	6.40
Dry distiller grains with soluble	—	9.14
Calcium salts of fatty acids[1]	—	1.01
Calcium carbonate	—	0.8
Calcium chloride, dehydrated	1.98	—
Larvicides[2]	0.08	0.04
Mycotoxin binder[3]	0.16	0.10
Sodium bicarbonate	—	1.01
Salt white	—	0.50
Magnesium oxide	—	0.16
Selenium product[4]	0.03	0.02
Biotin	—	0.40
Sodium selenite	—	0.01
Mineral and vitamin mix[5,6]	0.04	0.02
Vitamin ADE mix[7,8]	0.09	0.01
Vitamin E	0.03	0.01
Ionophore[9]	0.02	0.01
Chemical analysis		
DM%	51.1	55.9
NEL (Mcal/kg of DM)	1.67	1.80
CP (% DM)	13.5	17.7
NDF (% DM)	40.90	32.50
ADF (% DM)	23.20	18.3
Fatty acids (% DM)	2.58	3.03
MP-Lys (g/d)	83	155
MP-Met (g/d)	28	56
Lys:Met	2.96	2.77
DCAD (mEq/100 g)	−76	—

[1]EnerGII (Virtus Nutrition LLC, Corcoran, CA).

[2]ClariFly larvicide premix (0.67% diflubenzuron; Central Life Sciences).

[3]Mycosorb (Alltech Inc.).

[4]Sel-Plex 600 (Alltech Inc.).

[5]Close-up mix contained 223 g/kg calcium, 75 g/kg magnesium, 28 g/kg potassium, 39 g/kg sulfur, 15 g/kg manganese, 15,000 mg/kg zinc, 9,500 mg/kg iron, 2,500 mg/kg copper, 200 mg/kg iodine, 200 mg/kg cobalt, 66 mg/kg selenium, 227,273 IU/kg vitamin A, 136,364 IU/kg vitamin D_3, 636 IU/kg vitamin E.

[6]Fresh cow mix contained 70 g/kg calcium, 20 g/kg copper, 40 g/kg iron, 120 g/kg manganese, 210 g/kg zinc, 50 mg/kg cobalt, 3,000 mg/kg iodine.

[7]Close-up mix contained 3,500 IU/kg vitamin A, 950 IU/kg vitamin D_3, 2,000 IU/g vitamin E.

[8]Fresh cow mix contained 5,448 kIU/kg vitamin A, 1,816 kIU/kg vitamin D_3, 9,080 IU/kg vitamin E.

[9]Rumensin 90 (Elanco Animal Health).

Feed and Milk Samples

Dry matter intake was measured daily. Individual ingredient samples were collected weekly and frozen at −20°C until chemical analysis. The samples were pooled monthly and shipped to Cumberland Valley Analytical Services (Waynesboro, PA) and analyzed for DM (AOAC International, 2000), CP (Leco FP-528 N Combustion Analyzer, Leco Corp., St. Joseph, MO), starch (Hall, 2009), NDF (Van Soest et al., 1991), lignin (Goering and Van Soest, 1970), ADF (AOAC International, 2000), crude fat (AOAC International, 2006), ash (AOAC In-

ternational, 2000), and minerals (AOAC International, 2006). The values for NEL, DM, CP, ADF, NDF, FA, and DCAD were estimated using the NASEM (2021) model with actual BW, BCS, milk production, and milk composition as inputs (Table 1).

Cows were milked twice daily (0100 and 1300 h), and milk weights were automatically recorded at each milking. Consecutive milk samples taken at 0100 and 1300 h were collected 1 d/wk during the experimental period. Milk samples from each milking session were preserved (800 Broad Spectrum Microtabs II, D & F Control Systems Inc., San Ramon, CA) and stored at 4°C until shipping to Lancaster DHIA (Manheim, PA). Milk samples were analyzed for fat, protein, lactose, MUN, and SCC. Milk yield from each milk sample collection was used to calculate the yields of milk components and then back calculate their concentrations in milk on that day. The mean concentration of milk components and the mean milk yield of each week were used to calculate yields of milk components and ECM per week. Based on milk sample analysis, ECM (kg/d) was calculated weekly as follows: ECM = (12.51 × kg of fat/d) + (7.88 × kg of true protein/d) + (5.32 × kg of lactose/d) (NASEM, 2021; Hall, 2023).

Energy balance (**EB**) was calculated for each cow using equation 20-327 in NASEM (2021). The net energy intake (**NEI**) was determined using daily DMI multiplied by the NEL density of the diet. The NEM was calculated as $0.10 \times BW^{0.75}$ (NASEM, 2021). Requirements of NEL for milk production ($\mathbf{NE_{Milk}}$) were calculated as NE_{Milk} = (9.29 × fat yield) + (5.85 × true protein yield) + (3.93 × lactose yield). The NEL for gestation (**NEP**) was calculated using equation 3-18 in NASEM (2021) as NEP = ($GrUter\_Wt_{gain}$) × 4.16, where $GrUter\_Wt_{gain}$ is the gravid uterine wet tissue deposition gain estimated with equations 3-15 and 3-17 in NASEM (2021) as GrUter_Wtgain = [0.0243 − (0.0000245 × Day of gestation)] × (calf birth weight × 1.825). The equation used to calculate postpartal EB (EBPOST) was EBPOST (Mcal/d) = NEI − (NEM + NEL) and EBPOST (as % of requirements) = [NEI/(NEM + NE_{Milk})] × 100.

Blood Collection and Analyses

Blood was sampled from the coccygeal vein using a 21-gauge BD Vacutainer Eclipse needle (Becton Dickinson, Franklin Lakes, NJ) twice a week before the morning feeding from −21 to 30 relative to parturition. For analysis purposes, samples were specifically analyzed at −21, −10, 2, 7, 14, and 21 DIM. Samples were collected into evacuated tubes (BD Vacutainer, Becton Dickinson, Franklin Lakes, NJ) containing either clot activator or lithium heparin for serum and plasma, respectively. After blood collection, tubes with lithium heparin were placed on ice, and tubes with clot activator were kept at 21°C until centrifugation. Serum and plasma were obtained by centrifugation at 1,300 × *g* for 15 min at 21°C and 4°C, respectively. Aliquots of serum and plasma were frozen at −80°C until further analysis.

Serum or plasma samples were analyzed for glucose (catalog no. 99703001, Fujifilm Medical Systems, Valhalla, NY), BHB (catalog no. 700190, Cayman Chemical, Ann Arbor, MI), nonesterified fatty acids (**NEFA**; catalog no. 99934691; Fujifilm Medical Systems Valhalla, NY), insulin (Bovine Insulin ELISA; catalog no. 10120101; Uppsala, Sweden), GPx (catalog no. 703102, Cayman Chemical, Ann Arbor, MI), muscle mass catabolism (i.e., urea), inflammation (i.e., albumin, globulin, ceruloplasmin, haptoglobin, myeloperoxidase [**MPO**]), liver function (e.g., total bilirubin, cholesterol, glutamic-oxaloacetic transaminase [**GOT**], GGT, and paraoxonase), ROM, ferric reducing antioxidant power (**FRAP**), and total thiol groups of plasma (**SHp**) using commercial kits (Trevisi et al., 2012; Mezzetti et al., 2019).

Liver Sample Collection and Analysis

Liver samples were collected via puncture biopsy for all cows in the experiment under local anesthesia at ~1000 h on d −8 ± 3.2 d, 7, and 21 relative to parturition. Briefly, the skin was shaved, and then the ultrasound probe was inserted between the last and penultimate intercostal spaces (count from the back) of the right rib to locate the liver. After disinfection of the skin with alcohol and iodine 10%, 10 mL of 2% lidocaine (catalog no. 13985-222-05, Vet One, Boise, ID) was applied to anesthetize both the skin and body wall. A stab incision (~2 cm) was made through the skin and muscle in the right intercostal space using a no. 10 blade, and an 18-gauge × 10.2-cm bone marrow probe (Monoject, catalog no. 8881-247087, Medtronic, Minneapolis, MN) was inserted through the incision and into the liver to obtain ~1 g of liver. Vetasan ointment (chlorhexidine gluconate 4%; catalog no. 55001-1, Kinetic VET, Lexington, KY) was applied over staples to prevent infection. Samples were rinsed with saline solution and flash-frozen immediately in liquid N, followed by storage at −80°C until further analysis for concentration of triacylglycerides (**TAG**), total GSH, oxidized GSH (**GSSG**), reduced GSH, ROM (catalog no. STA-347, Cell Biolabs Inc., San Diego, CA), GGT (catalog no. ab241029; Abcam, Cambridge, UK), and GPx activity (catalog no. 703102, Cayman Chemical, Ann Arbor, MI). Health parameters, including rectal temperature, feed intake, and incision appearance, were monitored for 3 d after each biopsy, and surgical skin staples were removed 5 d after the biopsy. All cows remained clinically healthy during the study.

TAG and GSH Assay

The TAG levels were measured according to the method described by Zhou et al. (2016) with some adaptations. Briefly, 40 mg of liver tissue was homogenized in 0.5 mL of PBS/10 m*M* EDTA and centrifuged at 10,000 × *g* for 1 min at 4°C. Subsequently, 50 µL of the supernatant was loaded into a glass tube and 2 mL of isopropanol-hexane-water (80:20:2 vol/vol) was added to each sample. The tube was covered with aluminum foil, and the mixture was incubated for 30 min at room temperature. An aliquot of 500 µL of hexane-diethyl ether (1:1) was added to each sample followed by vortexing and incubating for 10 min at room temperature (protected from light). Next, 1 mL of water was added to each sample to separate the lipid phase, and the mixture was vortexed. Samples were incubated and covered with aluminum foil for 20 min at room temperature. The organic phase was then aspirated and placed into glass vials before evaporation under a stream of N gas. An 8-point TAG standard (catalog no. 23-666-422, Fisher Scientific Inc.) was prepared with Infinity TG reagent (catalog no. TR22421I, Fisher Scientific Inc.). A total of 450 µL of Infinity TG reagent was added to each tube, followed by vortexing and incubation at 37°C in a shaker for 15 min. Then, 120 µL of this sample mixture was pipetted into a flat-bottom 96-well microplate and the absorbance was determined at 540 nm using a microplate reader. The concentration of TAG was calculated from the standard curve.

Total and oxidized glutathione levels were measured in the liver at −8, 7, and 21 d relative to parturition using a commercial kit (catalog no. MAK440, Sigma Aldrich). Briefly, 40 mg of liver tissue was homogenized in 200 µL of cold buffer containing 50 m*M* sodium phosphate monobasic (pH 7) and 1 m*M* EDTA using one 5-mm stainless steel bead (catalog no. 69989, Qiagen, Hilden, Germany) and homogenized in a Qiagen TissueLyser LT (catalog no. 85600, Qiagen, Hilden, Germany) for 1 min. Next, 25 µL of supernatant was deproteinated using 65 µL of 5% wt/vol metaphosphoric acid. A total of 18 µL of clear supernatant was taken and mixed with 732 µL of 1× assay buffer. A 4-point GSH standard was prepared with the GSH standard. A total of 200 µL of GSH standard and samples were pipetted into a flat-bottom 96-well plastic microplate and 100 µL of the working reagent (1× assay buffer, glutathione reductase enzyme, NADPH, and 5,5′-dithio-bis2-nitrobenzoic acid) was subsequently added. Absorbance was taken immediately and after 10 min at 412 nm. To measure GSSG, 20 µL of scavenger was added to the cold buffer before homogenization. Reduced GSH was calculated as follows: reduced GSH = total GSH − (2 × GSSG).

RNA Isolation and Reverse Transcription-qPCR

Total RNA was extracted from liver tissue using Trizol (catalog no. 15596018, Invitrogen, Carlsbad, CA) reagent in combination with the RNeasy Plus Mini Kit (Qiagen; catalog no. 74134; Hilden, Germany), following the manufacturer's instructions with some modifications. Briefly, 200 mg of liver tissue immersed in Trizol was transferred to a 2 mL RNase-free O-ring tube containing one 5-mm stainless steel bead (catalog no. 69989; Qiagen, Hilden, Germany) and homogenized in the Qiagen TissueLyser LT (catalog no. 85600; Qiagen, Hilden, Germany) for 1 min. After homogenization, the lysate was transferred to a 2-mL RNase/DNase-free microtube, and 200 µL of phenol:chloroform (catalog no. AM9730, Invitrogen, Carlsbad, CA) at 4°C was added to isolate the RNA from the organic phase. After centrifugation at 13,000 × *g* for 15 min at 4°C, the upper phase was transferred into a new 2-mL RNase-free microtube. The remaining steps of the protocol were performed in the QIAcube machine (catalog no. 9002864, Qiagen, Hilden, Germany) according to the manufacturer's recommendation. The RNA quantity and purity were measured using a Nanodrop spectrophotometer (NanoDrop Technologies, Wilmington, DE). The RNA quantity for all liver samples was 667.9 ± 207.9 ng/µL, and the purity of RNA (absorbance at 260 nm:280 nm) was 1.96 ± 0.04 for the samples. The RNA integrity was assessed using the Tape Station (Agilent Technologies, Santa Clara, CA), and the final RNA integrity number was 8.0 ± 0.8.

The RNA extracted from liver tissue was used for real-time quantitative PCR (**qPCR**) analysis. Complementary DNA synthesis was performed according to Osorio et al. (2014a), with some changes. The cDNA was synthesized using 100 ng of RNA, 1 µL of random primers (Invitrogen Corp., Waltham, MA), and 9 µL of DNase/RNase-free water (HyClone, UltraPure, Cytiva; catalog no. SH3053803; Marlborough, MA). The mixture was incubated at 65°C for 5 min and kept on ice for 5 min. Next, 9 µL of master mix composed of 4 µL of 5× reaction buffer, 1 µg of dT18 (catalog no. 51-01-15-07, Integrated DNA Technologies, Coralville, IA), 2 µL of 10 mmol/L dNTP mix (catalog no. 18427088, Invitrogen Corp., Carlsbad, CA), 0.25 µL (200 U/µL) of RevertAid Reverse Transcriptase (catalog no. EP0441, Thermo Scientific, Waltham, MA), 0.125 µL of RNase inhibitor (20 U/µL, Promega, Madison, WI), and 1.625 µL of DNase/RNase-free water (HyClone, UltraPure) was added. The reaction was performed in an Eppendorf Mastercycler Gradient using the following temperature program: 25°C for 5 min, 42°C for 120 min, and 70°C for 5 min. The real-time quantitative PCR was performed according to Rosa et al. (2021) using a QuantStudio 6 Flex Real-Time PCR System (Applied

Table 2. Frequency of health problems in transition cows classified by prepartal liver glutathione (GSH) content as high (HGSH), medium-high (MHGSH), medium-low (MLGSH), and low (LGSH)

	Group				
Event	LGSH (n = 15)	MLGSH (n = 15)	MHGSH (n = 15)	HGSH (n = 15)	*P*-value[1]
Ketosis[2]	3[b]	10[a]	4[b]	5[ab]	0.04
Mastitis[3]	3	0	1	0	0.09
Retained placenta[4]	1	3	1	2	0.62
Hypocalcemia[5]	2	1	0	1	0.56

[a,b]Mean values with different superscripts differ ($P < 0.05$).

[1]Health data were analyzed with the FREQ procedure of SAS with chi-square tests of association.

[2]Defined as cows having ketones >2.1 mmol/L measured with Precision Xtra analyzer (Abbott) and treated with oral propylene glycol or intravenous dextrose.

[3]Initially determined with California Mastitis Test and confirmed via laboratory analysis.

[4]Defined as fetal membranes retained >24 h postpartum.

[5]Low milk colostrum production, lethargy, muscle tremors.

Biosystems, Waltham, MA) with the following conditions: 2 min at 50°C, 10 min at 95°C, and 40 cycles with 15 s at 95°C followed by 1 min at 60°C. A dissociation curve (gradient from 95°C to 60°C to 95°C for 15 s) was performed to check for amplicon quality.

Details about the primer sequence information and sources can be found in Supplemental Table S1 (see Notes). The final gene expression data were normalized using the geometric mean of *GAPDH*, *RPS9*, and *UXT*, which have previously been verified as suitable internal control genes (Bionaz and Loor, 2007). The target genes measured are described in Supplemental Table S1 and are associated with the glutathione cycle, specifically glutamate-cysteine ligase (*GCL*), γ-glutamylcyclotransferase (*GGCT*), γ-glutamyltransferase (*GGT*), glutathione-disulfide reductase (*GSR*), glutathione synthetase (*GSS*), and 5-oxoprolinase (*OPLAH*). Additionally, oxidative stress–related genes such as glutathione peroxidase-1 (*GPX1*) and nuclear factor erythroid 2-related factor 2 (*NFE2L2*) are included, along with the enzyme glucose-6-phosphate dehydrogenase (*G6PD*), which is involved in glucose metabolism.

Statistical Analysis

Continuous data were analyzed by ANOVA with linear mixed-effects models using the PROC MIXED of SAS according to the following model:

$$Y_{ijk} = \mu + M_i + T_j + P_k + MT_{ij} + e_{ijk},$$

where Y_{ijk} = dependent, continuous variable; μ = overall mean; M_i = fixed effect of group (i = HGSH, MHGSH, MLGSH, and LGSH); T_j = fixed effect of time (j = days or weeks); P_k = fixed effect of parity; MT_{ij} = interaction between group and time (group × time); and e_{ijk} = residual error. Cow nested within group was used as the random effect. Least squares means separation between time points was performed using the PDIFF statement in SAS.

Repeated measures analysis for equally spaced data (e.g., milk yield, BW, and DMI) was modeled with autoregressive or heterogeneous autoregressive covariance structures and selected based on the least Bayesian information criterion value. A priori orthogonal contrasts were analyzed with the CONTRAST statement in SAS to determine linear and quadratic effects over GSH group levels. Because the liver GSH concentrations were not equally spaced across groups, SAS Proc IML was used to generate coefficients for linear and quadratic orthogonal contrasts. Blood and liver biomarker data were analyzed at various time points that were not equally spaced; therefore, an exponential correlation covariance structure SP (POW) was used for repeated measures. Blood biomarkers were log-scale transformed if needed to comply with a normal distribution of residuals.

The covariate of the previous 305-d milk yield was maintained in the model for all variables for which it was significant ($P < 0.05$). The parity effect was removed from the model any time it was nonsignificant ($P > 0.05$). The CORR procedure of SAS was used to test the Pearson correlation coefficient (r) among liver GSH concentration at −8 DIM, prepartal EB and NEI, blood biomarkers at −10 DIM, and mean concentration of blood biomarkers from 2 to 21 DIM. Gene expression data were normalized by logarithmic transformation before statistical analysis. Health data were analyzed with the FREQ procedure of SAS with chi-square tests of association (Table 2). Statistical significance was declared at $P \leq 0.05$, and trends at $P \leq 0.10$.

Table 3. Association of prepartal liver glutathione (GSH) concentration with feed intake parameters, BW, BCS, and energy balance parameters in transition dairy cows classified as high (HGSH), medium-high (MHGSH), medium-low (MLGSH), and low (LGSH)

	Group					*P*-value[1]			
Item[2]	LGSH (n = 15)	MLGSH (n = 15)	MHGSH (n = 15)	HGSH (n = 15)	SEM[3]	Group	Time	G × T	Linear
Prepartum[4]									
DMI (kg/d)	13.3	12.3	13.3	14.5	0.57	0.07	<0.01	0.69	0.07
BW (kg)	827.5	778.5	787.1	814.5	16.00	0.03	<0.01	0.88	0.74
BCS (1 to 5)	3.40	3.36	3.37	3.53	0.09	0.40	0.65	0.76	0.21
DMI (% of BW)	1.55	1.60	1.65	1.74	0.09	0.48	<0.01	0.53	0.12
EB (Mcal/d)	−1.55	−2.52	−0.65	1.11	0.99	0.05	<0.01	0.56	0.02
EB (%)	92.7	87.9	97.1	105.5	4.82	0.05	<0.01	0.57	0.03
NEM (Mcal/kg)	15.4	14.7	14.8	15.2	0.19	0.03	<0.01	0.89	0.76
NEI (Mcal/kg)	19.6	18.4	19.7	21.8	0.89	0.06	<0.01	0.53	0.04
NEP (Mcal/kg)	6.0	6.2	6.0	6.2	0.14	0.44	<0.01	0.46	0.42
Postpartum[5]									
DMI (kg/d)	21.3	20.6	20.9	22.6	0.69	0.19	<0.01	0.28	0.14
BW (kg)	731.5	703.7	697.5	742.5	13.42	0.02	<0.01	0.68	0.43
BCS (1 to 5)	3.00	3.02	2.99	3.16	0.05	0.10	<0.01	0.41	0.05
DMI (% of BW)	3.00	3.16	3.16	3.20	0.09	0.41	<0.01	0.67	0.16
EB (Mcal/d)	−17.1	−15.9	−17.7	−16.4	1.44	0.80	0.06	0.27	0.91
EB (%)	65.5	67.5	64.6	66.0	2.84	0.83	<0.01	0.28	0.94
NE_{Milk} (Mcal/kg)	37.3	36.7	38.0	40.2	1.40	0.29	<0.01	0.24	0.09
NEM (Mcal/kg)	14.1	13.7	13.6	14.2	0.20	0.01	<0.01	0.68	0.41
NEI (Mcal/kg)	34.8	33.8	34.3	37.1	1.15	0.19	<0.01	0.68	0.12

[1]G × T = interaction of group × time. Linear = *P*-value associated with a linear effect over the prepartal liver GSH groups. Prepartal and postpartal BW and prepartal and postpartal NEM had a quadratic effect ($P \leq 0.01$).

[2]EB = energy balance; NEI = net energy of intake; NEP = net energy for pregnancy; NE_{Milk} = net energy for milk synthesis.

[3]Largest SEM.

[4]Prepartum parameters were analyzed from −21 d to calving.

[5]Postpartum parameters were analyzed from calving to 30 DIM.

RESULTS

Health

Among the health problems recorded during the experiment, a significant effect ($P = 0.04$) for ketosis events was observed, with MLGSH cows experiencing a higher ($P \leq 0.03$) incidence of ketosis than MHGSH and LGSH groups. Similarly, a trend ($P = 0.06$) for greater incidence of ketosis in MLGSH in comparison with HGSH was observed. Additionally, a trend ($P = 0.09$) for mastitis events was noted, in which LGSH cows had more incidents of mastitis compared with the other groups (Table 2).

Peripartal DMI, BW, BCS, and EB

We observed a negative quadratic effect ($P \leq 0.01$) on prepartal and postpartal BW across the GSH groups (Table 3). This was reflected in LGSH and HGSH cows having more BW than MLGSH and MHGSH before and calving (Figure 1E and 1F, respectively). A linear increase ($P \leq 0.03$) in prepartal EB (in either Mcal/d or percentage) was observed as prepartal liver GSH increased from LGSH to HGSH (Figure 1G). The negative quadratic effect observed in prepartal and postpartal BW could be associated with the negative quadratic effect ($P \leq 0.01$) observed in NEM before and after calving across the GSH groups. A linear increase ($P = 0.05$) in postpartal BCS was observed, where postpartal BCS increased as prepartal liver GSH increased across groups. The linear increase in prepartal EB could be associated with both a linear increase ($P = 0.04$) in prepartal NEI and the trend ($P = 0.07$) for a linear increased in prepartal DMI as prepartal liver GSH increased across groups to LGSH and MHGSH (Table 3). We observed a trend ($P = 0.09$) for a linear increase in postpartal NE_{Milk} as prepartal GSH levels increased from LGSH to HGSH. Prepartal and postpartal DMI (% of BW), postpartal DMI, prepartal BCS, and postpartal EB were not affected ($P \geq 0.19$) by linear or quadratic effects.

Milk Production and Composition

A group × time interaction (**G × T**; $P = 0.04$) was observed for milk protein yield, which was reflected in greater ($P \leq 0.03$) milk protein yield in the HGSH group compared with other groups at 2, 3, and 4 wk postpartum (Table 4; Figure 2D). A trend ($P = 0.09$) for a linear increase in milk yield (from 42.1 to 46.7 kg/d) as GSH levels increased from LGSH to HGSH. Similarly, a lin-

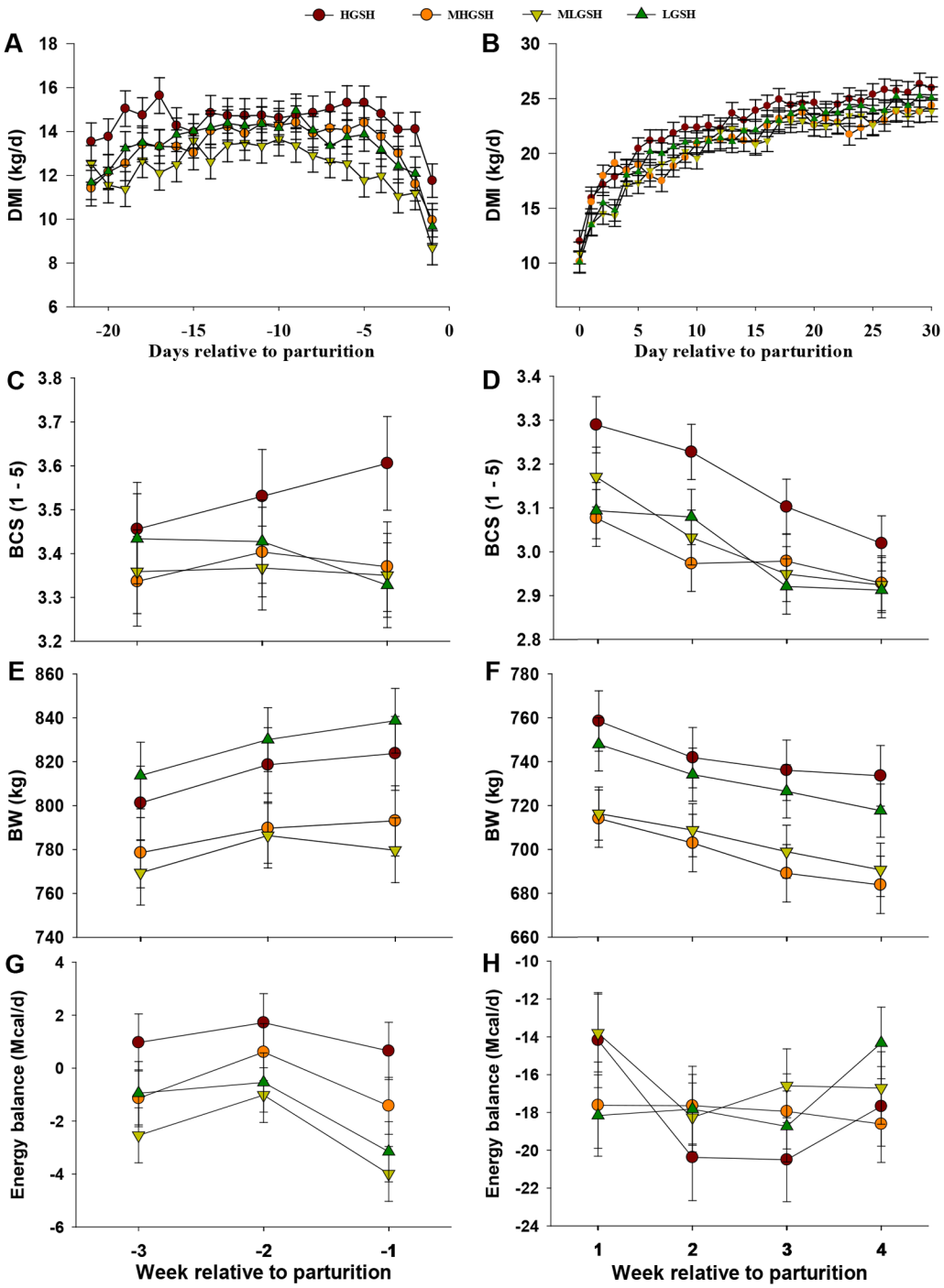

Figure 1. Prepartal (left side) and postpartal (right side) DMI (A, B), BCS (C, D), BW (E, F), and EB (G, H) in dairy cows retrospectively grouped (n = 15/treatment) based on liver GSH concentration at −8 d before calving into HSGH, MHGSH, MLGSH, and LGSH concentration. Values are means, and SE are represented by vertical bars.

ear increase ($P = 0.05$) in ECM (from 50.2 to 54.7 kg/d) was observed when liver GSH increased from LGSH to HGSH groups (Figure 2B). Milk fat yield, SCC, lactose percentage, and MUN were not affected ($P \geq 0.34$) by linear or quadratic effects.

Blood and Liver Metabolites

We observed a G × T interaction for blood biomarkers, including whole blood BHB ($P = 0.05$), cholesterol ($P = 0.01$), GOT ($P = 0.04$), and FRAP ($P = 0.05$). The G × T

Table 4. Association of prepartal liver glutathione (GSH) concentration with lactation performance and feed efficiency parameters in transition dairy cows classified as high (HGSH), medium-high (MHGSH), medium-low (MLGSH), and low (LGSH)

	Group					*P*-value[1]			
Item	LGSH (n = 15)	MLGSH (n = 15)	MHGSH (n = 15)	HGSH (n = 15)	SEM[2]	Group	Time	G × T	Linear
Milk yield (kg/d)	42.1	44.7	41.2	46.7	1.48	0.05	<0.01	0.97	0.09
ECM (kg/d)	50.2	49.5	51.3	54.7	1.85	0.19	<0.01	0.22	0.05
Milk composition									
Milk fat (%)	6.00	5.31	6.21	5.39	0.18	<0.01	<0.01	0.26	0.16
Milk protein (%)	3.44	3.22	3.45	3.40	0.07	0.04	<0.01	0.23	0.72
Lactose (%)	4.78	4.81	4.81	4.92	0.08	0.60	<0.01	0.42	0.20
Milk fat yield (kg/d)	2.33	2.24	2.44	2.39	0.10	0.48	<0.01	0.29	0.40
Milk protein yield (kg/d)	1.33	1.31	1.33	1.46	0.05	0.10	<0.01	0.04	0.04
SCC[3]	2.88	2.20	2.68	1.83	0.43	0.34	<0.01	0.63	0.15
MUN (mg/dL)	11.16	11.68	11.94	12.14	0.52	0.54	<0.01	0.41	0.17
Efficiency									
Milk/DMI	1.93	1.98	1.86	1.94	0.07	0.60	<0.01	0.36	0.80
ECM/DMI	2.47	2.35	2.48	2.40	0.10	0.73	0.01	0.29	0.83

[1]G × T = interaction of group × time. Linear = *P*-value associated with a linear effect over the prepartal liver GSH groups. None of the parameters had a quadratic effect ($P \geq 0.14$).

[2]Largest SEM.

[3]Somatic cell counts were transformed to $\log_{10}$.

observed in whole blood BHB was attributed to greater ($P \leq 0.01$) whole blood BHB in MLGSH cows compared with all other groups at 5 DIM (Table 5; Figure 3B). This effect in whole blood BHB was confirmed by a positive quadratic effect ($P = 0.04$) in plasma BHB and a trend ($P = 0.10$) for a positive quadratic effect in whole blood BHB. In the case of cholesterol, the G × T was associated with greater ($P \leq 0.05$) cholesterol in HGSH cows compared with all other treatments at 21 DIM (Figure 3C). The G × T in GOT was reflected in lower ($P < 0.01$) levels in the HGSH group compared with MHGSH and MLGSH at 7 DIM, followed by lower ($P < 0.01$) GOT in HGSH compared with LGSH at 14 DIM (Figure 3D). These effects were reflected in a trend ($P = 0.07$) for a positive quadratic effect in GOT across GSH groups. The G × T in FRAP was reflected in lower ($P = 0.03$) FRAP in the LGSH group compared with MLGSH at −10 DIM, followed by greater ($P = 0.03$) FRAP in the LGSH group compared with other groups at 14 DIM (Figure 3E). A linear increase ($P < 0.01$) in SHp from 473.6 to 524.1 µmol/L was observed as prepartal liver GSH increased.

A linear increase ($P \leq 0.01$) in glucose (from 64.9 to 69.2 mg/dL) and insulin (from 0.15 to 0.21 ug/L) as prepartal GSH levels increased. No linear or quadratic effects ($P \geq 0.13$) were observed in blood biomarkers, including NEFA, urea, total bilirubin, GGT, paraoxonase, albumin, ceruloplasmin, haptoglobin, MPO, globulin, ROM, and GPx1.

We observed a G × T interaction ($P \leq 0.02$) for liver metabolites, including total GSH, GSSG, reduced GSH, and reduced GSH/GSSG ratio (Table 5). As expected, the G × T observed in total and reduced liver GSH was attributed to greater ($P \leq 0.01$) total and reduced liver GSH in the HGSH group compared with all other groups at −8 d relative to calving (Figure 4A and 4C). In contrast to HGSH, the LGSH group had lower total and reduced liver GSH when compared with all other groups at −8 d relative to calving. Additionally, the MHGSH group had greater ($P < 0.03$) total liver GSH compared with MLGSH and LGSH at −8 d relative to calving. At 7 DIM, the HGSH group had greater ($P = 0.05$) total and reduced GSH compared with LGSH. At 21 DIM, HGSH had greater ($P = 0.04$) levels of total GSH than those in the MLGSH and LGSH group (Figure 4A). Based on the design of this study, a linear effect ($P < 0.01$) on total and reduced GSH was expected, where total and reduced GSH increased linearly from the LGSH group to the HGSH group, which also contributed to an overall group effect ($P < 0.01$; Table 5). The G × T observed in GSSG was explained by greater ($P < 0.01$) GSSG in HGSH and MHGSH when compared with MLGSH and LGSH at −8 d before calving. The latter was followed by a lower ($P = 0.04$) GSSG in LGSH when compared with HGSH at 7 DIM (Figure 4B). Similar to total and reduced GSH, a linear effect ($P < 0.01$) was observed in GSSG, where GSSG concentrations increased from the LGSH group to the HGSH group (Table 5). The G × T observed in reduced GSH/GSSG ratio was associated with greater ($P = 0.03$) GSH/GSSG ratio in MLGSH cows compared with all other groups at −8 DIM (Figure 4D).

The group effect ($P = 0.03$) on liver GGT activity was attributed to a positive quadratic effect ($P < 0.01$) on liver GGT activity across GSH groups. Similar to liver GGT, a positive quadratic effect ($P = 0.03$) was

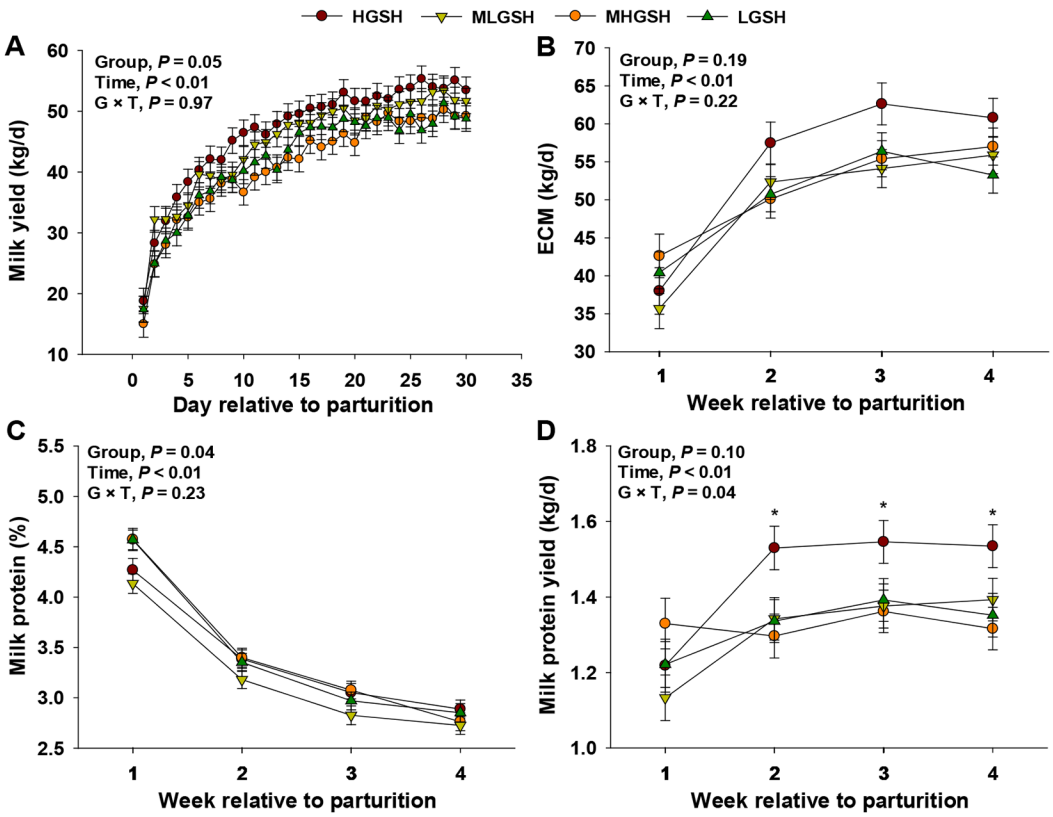

Figure 2. Milk yield through 30 DIM (A), weekly ECM (B), milk protein percentage (C), and milk protein yield (D) in dairy cows retrospectively grouped (n = 15/treatment) based on liver GSH concentration at −8 d before calving into HSGH, MHGSH, MLGSH, and LGSH. Mean separations between groups at a given time point were evaluated when a group × time (G × T) interaction ($P \leq 0.05$) was observed, and differences (*) were declared at $P \leq 0.05$. Values are means, and SE are represented by vertical bars.

observed in liver TAG across GSH groups. No linear or quadratic effects ($P \geq 0.17$) were observed for ROM and GPx activity in liver (Table 5).

Correlations Across Liver GSH, EB, NEI, and Blood Biomarkers

A positive correlation (r = 0.27; $P \leq 0.01$) was detected between prepartal EB and liver total GSH concentration (Table 6). Similar to prepartum EB, a positive correlation was observed between liver GSH and glucose (r = 0.26; $P = 0.04$), as well as insulin (r = 0.31; $P < 0.01$; Supplemental Figure S3C and S3D, respectively, see Notes). A negative correlation (r = −0.31; $P \leq 0.01$) was observed between the day relative to calving and liver total GSH concentration (Supplemental Figure S2, see Notes). A trend (r = 0.35; $P = 0.07$) for a positive correlation was observed between total liver GSH and NEI. Additionally, there was a positive correlation (r = 0.41; $P < 0.01$) between prepartal liver GSH and cholesterol. We found no significant ($P \geq 0.14$) correlation between prepartal liver GSH and any other metabolites evaluated at −10 DIM in this study.

Prepartal liver GSH was positively correlated with the mean concentration of blood insulin (r = 0.30; $P = 0.02$), cholesterol (r = 0.26; $P = 0.05$), and SHp (r = 0.41; $P < 0.01$) from 2 to 21 DIM (Supplemental Table S4, see Notes). Similarly, a trend (r = 0.22; $P = 0.09$) for a positive correlation between prepartal liver GSH and mean blood glucose from 2 to 21 DIM was observed (Supplemental Table S4).

Gene Expression

The mRNA expression of *GGCT* ($P < 0.01$), *GCLC* ($P = 0.05$), and *GSR* ($P = 0.01$) was altered in relation to prepartal liver GSH (Table 7). This was reflected in a linear upregulation ($P \leq 0.03$) of *GGCT*, *GCLC*, and *GSR* as prepartal GSH levels increased across groups. A trend ($P = 0.06$) for a linear effect on *GGT* expression was observed as prepartal liver GSH increased across groups. A positive quadratic effect was observed for the mRNA

Table 5. Peripartal blood and liver biomarkers in transition cows classified by prepartal liver glutathione (GSH) content as high (HGSH), medium-high (MHGSH), medium-low (MLGSH), and low (LGSH)

	Group					*P*-value[1]			
Item[2]	LGSH (n = 15)	MLGSH (n = 15)	MHGSH (n = 15)	HGSH (n = 15)	SEM[3]	Group	Time	G × T	Linear
Metabolism									
NEFA[4] (mEq/L)	0.41	0.43	0.41	0.37	0.10	0.50	<0.01	0.56	0.26
BHB (mmol/L)	0.57	0.72	0.59	0.48	0.06	0.04	<0.01	0.54	0.11
Whole blood BHB[5] (mmol/L)	1.17	1.57	1.15	1.13	0.12	0.01	<0.01	0.01	0.29
Glucose[4] (mg/dL)	64.9	62.6	66.3	69.2	1.2	<0.01	<0.01	0.24	<0.01
Insulin[4] (µg/L)	0.15	0.14	0.19	0.21	0.15	0.03	<0.01	0.29	0.01
Urea (mmol/L)	3.91	4.04	3.73	4.00	0.20	0.54	<0.01	0.11	0.92
Liver function									
Total bilirubin[4] (µmol/L)	2.05	1.93	2.10	1.90	0.15	0.80	<0.01	0.42	0.65
Cholesterol (mmol/L)	2.26	2.28	2.27	2.45	0.13	0.59	<0.01	0.01	0.24
GGT (U/L)	21.7	21.2	22.1	20.8	1.07	0.81	<0.01	0.35	0.66
GOT (U/L)	104.8	109.3	111.6	100.4	4.39	0.27	<0.01	0.04	0.47
Paraoxonase (U/mL)	77.7	79.1	77.05	85.5	3.48	0.30	<0.01	0.54	0.14
Inflammation									
Albumin (g/L)	34.8	34.3	34.6	34.7	0.55	0.87	<0.01	0.23	0.98
Ceruloplasmin (µmol/L)	2.85	2.72	2.78	2.73	0.10	0.82	<0.01	0.80	0.55
Haptoglobin[4] (g/L)	0.20	0.22	0.28	0.23	0.16	0.13	<0.01	0.76	0.22
MPO (U/L)	474.6	465.4	484.1	463.9	15.20	0.75	<0.01	0.43	0.77
Globulin (g/L)	37.8	35.1	36.4	36.5	0.88	0.16	<0.01	0.17	0.55
Oxidative stress									
ROM (mg H_2O_2/100 mL)	16.8	16.1	16.4	16.3	0.59	0.73	<0.01	0.49	0.58
FRAP (µmol/L)	144.7	147.5	143.8	146.7	2.47	0.65	<0.01	0.05	0.76
GPx1 (nmol/min/mL)	142.4	147.1	139.3	158.3	6.28	0.16	<0.01	0.20	0.11
SHp (µmol/L)	473.6	494.5	507.4	524.1	14.1	0.07	<0.01	0.09	<0.01
Liver									
Total GSH (nmol/mg)	0.83	1.09	1.26	1.74	0.10	<0.01	0.03	<0.01	<0.01
GSSG (nmol/mg)	0.07	0.09	0.13	0.17	0.01	<0.01	<0.01	<0.01	<0.01
Reduced GSH (nmol/mg)	0.66	0.93	0.99	1.37	0.07	<0.01	0.06	<0.01	<0.01
GHS/GSSG ratio[6]	14.7	15.3	12.6	11.2	0.25	0.56	0.04	0.02	0.32
TAG (% wet wt)	4.5	5.5	5.2	4.3	0.45	0.17	<0.01	0.31	0.64
GGT[7] (nmol/min per mL)	2,197.6	2,585.6	2,937.2	2,116.3	223.60	0.03	—	—	0.87
GPx1[8] (nmol/min per mL)	391.9	473.5	477.0	375.4	50.5	0.29	—	—	0.72
ROM[8] (RFU)	20.8	19.5	21.4	25.1	5.99	0.86	—	—	0.48

[1]G × T = interaction of group × time. Linear = *P*-value associated with a linear effect over the prepartal liver GSH groups. Plasma BHB, liver TAG, and liver GGT had a positive quadratic effect ($P \leq 0.03$). A trend ($P \leq 0.10$) for a positive quadratic effect was observed in whole blood BHB and plasma GOT.

[2]ROM = reactive oxygen metabolites; GPx1 = glutathione peroxidase; FRAP = ferric reducing antioxidant power; SHp = total thiol groups of plasma; GSSG = glutathione disulfide-oxidized; reduced GSH = GSHt – [2 × (GSSG)]; TAG = triacylglycerides.

[3]Largest SEM.

[4]Data were log-transformed before statistics and back-transformed means are presented. The SEM associated with log-transformed data is in the log scale.

[5]β-Hydroxybutyrate measured using a Precision Xtra machine (Abbott) in whole blood at 1, 3, 5, 7, 9, and 11 d relative to parturition.

[6]Calculated ratio of reduced GSH/GSSG. Data were log-transformed before statistics and back-transformed means are presented. The SEM associated with log-transformed data is in the log scale.

[7]Gamma-glutamyl transpeptidase (GGT) was measured in the liver at −8 d relative to calving.

[8]Glutathione peroxidase (GPx1) and ROM were measured in the liver at 7 d relative to calving. RFU = relative fluorescence units.

expression of *G6PD* and *NFE2L2* across prepartal liver GSH groups. No linear or quadratic effects ($P \geq 0.11$) were observed for the expression of the *GSS*, *OPLAH*, and *GPX1* genes.

DISCUSSION

Glutathione is a rich source of AA due to its tripeptide structure, γ-L-glutamyl-L-cysteinylglycine (Lu, 2013). It is a potent antioxidant present in all mammalian tissues, and it is primarily synthesized in the liver and is crucial during periods of high oxidative stress. The production of GSH depends on the availability of Cys. This nonessential AA can be derived from different sources, with Met serving as the primary precursor through the transsulfuration pathway. Because this pathway occurs particularly in the liver, Met is a key precursor and plays a crucial role in GSH synthesis (Lu, 2009). Previous studies conducted at the University of Illinois observed that supplementing transition dairy cows with RPM can

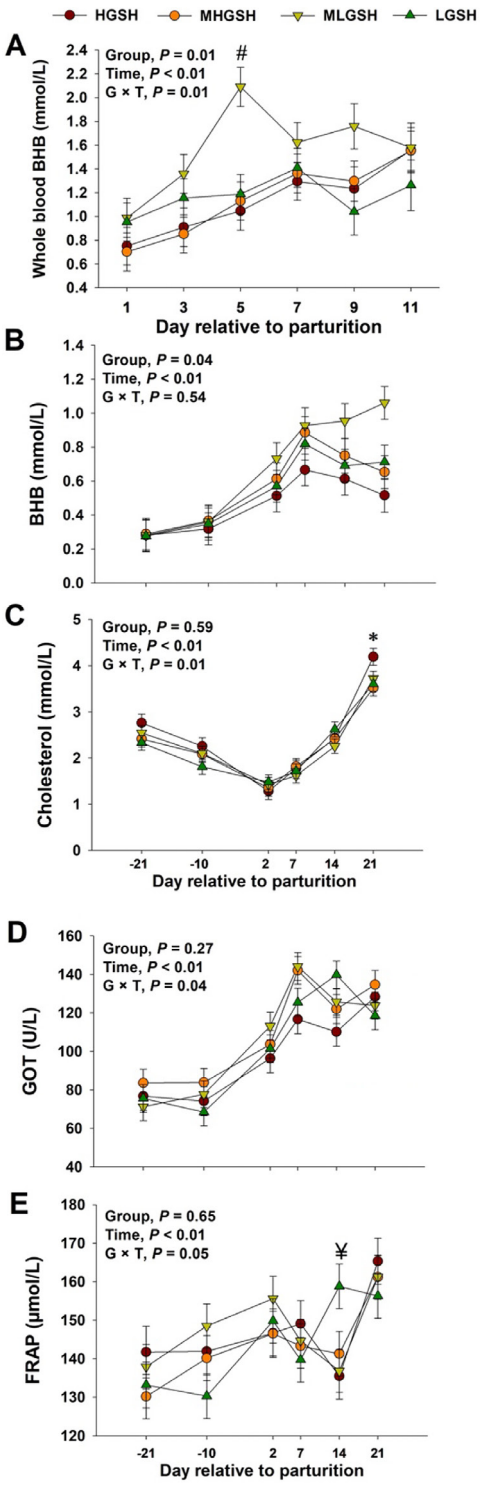

Figure 3. Whole blood BHB (A), BHB (B), cholesterol (C), GOT (D), and FRAP (E) in dairy cows retrospectively grouped (n = 15/treatment) based on liver glutathione (GSH) concentration at −8 d before calving into HSGH, MHGSH, MLGSH, and LGSH during the transition period. Mean separations between groups at a given time point were evaluated when a group × time (G × T) interaction ($P \leq 0.05$) was observed, and differences between MLGSH and all other groups (#), HGSH and all other groups (*), and LGSH and all other groups (¥) were declared at $P \leq 0.05$. Values are means, and SE is represented by vertical bars.

enhance the storage of liver GSH, especially before calving (Osorio et al., 2014b; Zhou et al., 2016; Batistel et al., 2018). However, there is limited evidence regarding the role of prepartal liver GSH and its effects on oxidative stress and immunometabolic markers in dairy cows. Therefore, the objective of our study was to determine potential mechanisms regulating the synthesis and degradation of prepartal liver GSH to better understand its prepartal accumulation in transition dairy cows and evaluate the association of prepartal liver GSH concentration with lactation performance, metabolism, and health outcomes during the postpartum period.

Connecting Body Condition Score and Energy Balance to Glutathione Levels

Through the transition period, dairy cows experience high nutrient requirements driven by the final stage of fetal growth and mammary gland development before calving and by lactogenesis after calving (Bauman and Currie, 1980; Bell, 1995; Sordillo and Aitken, 2009). This involves coordinating metabolic and endocrine processes to adapt to increased nutrient demands. However, a common issue during this period is a low energy intake in comparison to nutritional requirements (Drackley, 1999). As a result, cows often experience a negative energy balance (**NEB**) state during the transition period, when energy requirements to sustain lactation exceed energy intake from feed. To support the energy requirement for milk production, dairy cows mobilize lipids from adipose tissue in the form of NEFA, resulting in changes in BW and BCS during early lactation (Grummer, 1995; Drackley, 1999), as well as AA from muscle tissue (Bell, 1995).

Interactions between BCS and liver GSH have been seldom reported during the transition period of dairy cows. For instance, Bernabucci et al. (2005) observed that cows with high BCS before calving experienced greater fat mobilization and BCS loss after calving, along with increased plasma ROM, TBARS, and SHp levels, and reduced antioxidant capacity. The latter is evidenced by lower SOD activity and erythrocyte SH levels. Additionally, plasma GPx levels were higher after calving compared with prepartum levels, suggesting an increased requirement for a systemic antioxidant capacity after calving. However, it is important to note that Bernabucci et al. (2005) measured the GPx activity in plasma instead of total liver GSH. The GPx antioxidant mechanism is essential to reduce hydroperoxides utilizing GSH as a reducing agent. Bucktrout et al. (2021) retrospectively grouped cows as high (≥3.5) and normal (≤3.25) BCS during wk 4 before calving and observed a reduced liver GSH in high BCS cows. This effect was particularly evident at 30 d after calving, but not at 15 d before calving, suggesting that substantial differences in

Table 6. Correlation of prepartal liver total glutathione (GSH) with biopsy day relative to calving, prepartal EB and NEI, and blood biomarkers at −10 DIM

	GSH (nmol/mg)	
Item[1]	r	*P*-value
Prepartal variable		
Biopsy day relative to calving	−0.31	<0.01
Energy balance	0.27	<0.01
NEI	0.35	0.07
Energy metabolite		
Glucose (mg/dL)	0.26	0.04
Insulin (μL/L)	0.36	<0.01
Liver function		
Cholesterol (mmol/L)	0.41	<0.01

[1]NEI = net energy intake. There was no significant ($P \geq 0.20$) correlation between prepartal liver GSH and mean concentration of any other biomarker evaluated at −10 DIM.

BCS at 4 wk prepartum have less or no influence on liver GSH before calving.

In contrast to Bucktrout et al. (2021), our study identified a notable relationship between postpartal BCS and prepartal liver GSH levels. Specifically, cows with higher prepartal liver GSH exhibited an increase in BCS after calving, particularly in HGSH cows. The lack of differences in prepartal liver GSH between high and normal BCS groups observed by Bucktrout et al. (2021) could be explained by the positive EB maintained during late gestation in both groups. This positive EB could be interpreted as a minimum energy requirement to sustain an adequate liver GSH synthesis before calving. This is in agreement with our study, where we observed a negative EB in all groups except HGSH cows during late gestation. Furthermore, the observed effects on BCS were accompanied by a positive correlation between prepartal liver GSH and prepartal EB (Supplemental Figure S3A, see Notes), as well as a trend for a positive correlation between prepartal liver GSH and NEI (Supplemental Figure S3B). Taken together, future investigations ought to prioritize elucidating the interplay between dietary energy and hepatic GSH while considering the physiological limitations inherent to cows in late lactation.

Prepartal Liver Glutathione Associations with Lactation Performance

Our findings revealed that cows with high levels of GSH had increased milk production during the first 30 DIM, which highlights the role of GSH in supporting metabolic resilience and productivity during the transition period. Interestingly, the similar milk production between HGSH and MLGSH cows (46.7 vs. 44.7 kg/d, respectively) could be partially explained by the genetic merit for milk production of MLGSH cows, which was numerically higher than all other groups (Supplemental Figure S1, see Notes). There was a stronger association between prepartal liver GSH and ECM, where the linear increase in ECM as prepartal liver GSH increased could be related to GSH improvements on gluconeogenesis and supply of AA to the mammary gland.

The GSH cycle in the context of hepatocytes involves the export of GSH outside of the cell, where it can be extracellularly broken down by the membrane-associated enzyme, GGT, releasing the GSH constituent AA (i.e., Glu, Cys, and Gly), which can be transported back inside the cell via AA transporters (Bachhawat and Yadav, 2018). Once inside the cell, these AA can be used to resynthesize GSH or several other biological processes, including gluconeogenesis (Vázquez-Meza et al., 2023). Alternatively, GSH can be degraded by the cytoplasmatic ChaC-family of γ-glutamyl cyclotransferases that are glutathione-specific enzymes (Bachhawat and Yadav, 2018). The extent of the contribution of prepartal liver GSH–constitutive AA to gluconeogenesis during early lactation is unknown and perhaps negligible. Others have estimated that in general, only alanine has a significant contribution to the net liver release of glucose due to its role in the transfer of nitrogen from catabolized AA in muscle (Larsen and Kristensen, 2013). Alternatively, GSH could potentially influence gluconeogenesis via interactions with gluconeogenesis-related enzymes. For instance, Sáez et al. (1985) observed a decrease in the rate of gluconeogenesis when rat hepatocytes were depleted of GSH via substrates of GSH S-transferases or an inhibitor of glutamate-cysteine ligase. The hepatocytes were isolated from 48-h starved rats and incubated in 4 mL of Krebs–Henseleit saline. They further ascribe these results to GSH depletion affecting phosphoenolpyruvate carboxykinase and glycerol-3-phosphate activity. However, this needs further verification within the context of the bovine liver, where there is a higher dependency on propionate for gluconeogenesis. If prepartal liver GSH can influence gluconeogenesis in early lactation, it would be particularly advantageous immediately after calving, when insufficient DMI limits dietary nutrients for glucose precursors (e.g., propionate; NASEM, 2021). This notion was partially confirmed by the linear increase in glucose (Table 4) as prepartal liver GSH levels increased across groups. In line with these results are the linear increase in insulin as prepartal liver GSH increased across groups, presumably in response to the increase in glucose.

Atroshi and Sandholm (1982) observed significant arteriovenous differences in red blood cell (**RBC**) GSH levels in Finn sheep, associating these differences with increased milk production. They categorized the ewes into high-GSH and low-GSH groups based on RBC GSH levels. The authors observed that GSH concentrations were higher in the jugular vein than in the mammary

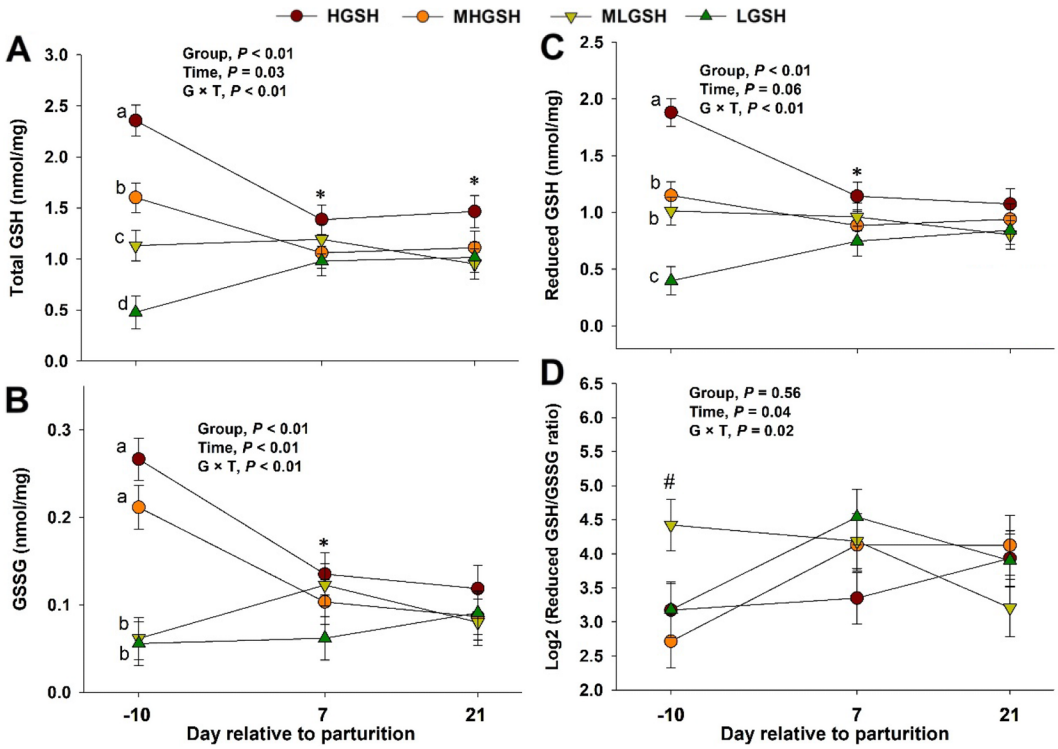

Figure 4. Effects of prepartal liver glutathione (GSH) concentration in liver total GSH (A), GSSG (B), reduced GSH (C), and $\log_2$-transformed ratio of reduced GSH/GSSG (D) measured or calculated throughout the peripartal period in dairy cows retrospectively grouped into HSGH, MHGSH, MLGSH, and LGSH concentrations. Mean separations between groups at a given time point were evaluated when a group × time (G × T) interaction ($P \leq 0.05$) was observed, and differences across groups (lowercase letters a–d), between HGSH and LGSH (*), and between MLGSH and all other groups (#) were declared at $P \leq 0.05$. Values are means, and the SEM is represented by vertical bars.

vein, suggesting a significant extraction of RBC GSH by the mammary gland. This effect, coupled with the greater milk production in the high-GSH group, indicates that RBC GSH may play a supportive role in milk production by supplying AA. These findings are supported by Pocius et al. (1981), who demonstrated that the mammary gland's uptake of GSH from whole blood provides a significant supply of AA necessary for milk synthesis. Later, Baumrucker (1985) clarified that mammary gland GGT and AA transporters work in concert to break down and take up constituent GSH-AA during lactation.

The mammary gland utilizes substantial amounts of plasma AA to synthesize milk protein (Baumrucker and Pocius, 1978). Therefore, even a small increase in milk protein synthesis correlates with improved AA net uptake by the mammary gland (Yoder et al., 2020). Pocius et al. (1981) reported a contrasting low mammary gland uptake of free plasma Cys and Glu, with substantial uptake of GSH. The GSH uptake by the mammary gland is facilitated by GGT, which cleaves the γ-glutamyl bond in GSH to release AA. Baumrucker and Pocius (1978) and Pocius et al. (1981) demonstrated that GGT activity is particularly high in bovine mammary tissue, which may reflect the enzyme's role in ensuring the availability of GSH constituent AA needed for milk protein synthesis.

Johnston et al. (2004) emphasized the importance of GGT activity in this process by investigating the effects of inhibiting this enzyme on milk protein synthesis in isolated ovine mammary cells using acivicin, a Gln analog, and GGT inhibitor. Their findings demonstrated that inhibiting GGT activity led to decreased milk protein synthesis, reinforcing the concept that mammary GGT may play a role in supplying the GSH-constituent AA necessary for milk protein synthesis. Similarly, research indicates the significance of GGT activity in the mammary gland of water buffaloes, with lactating buffaloes exhibiting greater GGT activity compared with their nonlactating counterparts (Pero et al., 2006).

In our study, the observed increase in milk protein yield in the HGSH group can primarily be ascribed to greater milk production, while maintaining a comparable milk protein percentage to other groups. This suggests that HGSH cows relied not only on the gluconeogenic activity of GSH-constituent AA but also had a sufficient supply of these AA to maintain milk protein synthesis. Although GSH plays an important role in neutralizing

Table 7. Changes in hepatic relative mRNA abundance of genes related to the glutathione (GSH) cycle, glucose metabolism, and oxidative stress at −8 d relative to calving in transition cows classified according to their prepartal liver GSH as high (HGSH), medium-high (MHGSH), medium-low (MLGSH), and low (LGSH) GSH

	Group					*P*-value[1]	
Gene[2]	LGSH	MLGSH	MHGSH	HGSH	SEM[3]	Group	Linear
GSH metabolism							
GCLC	−0.39	−0.36	0.02	−0.08	0.13	0.05	0.03
GGCT	−0.69	−0.51	−0.21	−0.29	0.10	<0.01	<0.01
GGT	−0.32	−0.24	−0.02	−0.04	0.13	0.19	0.06
GSR	−0.67	−0.40	−0.23	−0.16	0.12	0.01	<0.01
GSS	−0.40	−0.49	−0.33	−0.26	0.11	0.37	0.20
OPLAH	−0.37	−0.49	−0.48	−0.50	0.09	0.68	0.31
Glucose metabolism							
G6PD	−0.48	−0.36	−0.13	−0.40	0.10	0.11	0.41
Oxidative stress							
GPX1	−0.19	−0.33	−0.20	−0.21	0.12	0.73	0.89
NFE2L2	−0.25	−0.18	−0.06	−0.31	0.09	0.09	0.63

[1]Linear = *P*-value associated with a linear effect over the prepartal liver GSH groups. The mRNA expression of *G6PD* and *NFE2L2* had a quadratic effect ($P \leq 0.04$).

[2]Gene expression data were normalized by logarithmic transformation before statistical analysis. *GCLC* = glutamate-cysteine ligase, catalytic subunit; *GGCT* = γ-glutamyl cyclotransferase; *GGT* = γ-glutamyl transferase; *GSR* = glutathione-disulfide reductase; *GSS* = glutathione synthase; *OPLAH* = 5-oxoprolinase; *G6PD* = glucose-6-phosphate dehydrogenase; *GPX1* = glutathione peroxidase 1; *NFE2L2* = nuclear factor erythroid 2-related factor 2.

[3]Largest SEM.

oxidative stress, these findings highlight the positive impact of prepartal liver GSH on lactation performance by providing a source of gluconeogenic AA; however, the extent of AA supply to the mammary gland by liver GSH needs further validation.

The Role of Glutathione in the Homeorhetic Regulation of Blood Biomarkers and Liver Function

During the transition period, cows experience various adaptations that enable coordinated metabolic control to support the physiological state of body tissues, a process known as homeorhetic regulation (Baumgard et al., 2017). These adaptations are essential for maintaining optimal metabolic function during this critical phase, which is important for a successful transition. As a result of shifts in metabolic status, ruminants rely on the mobilization of lipids and proteins to meet their nutritional demands. The breakdown of TAG from body reserves generates NEFA and glycerol, which the organism utilizes to compensate for the energy deficit (Ingvartsen, 2006). As fat mobilization increases, excess NEFA levels can overwhelm the liver, exceeding its capacity to fully oxidize fatty acids for energy. This results in an increased production of ketone bodies, primarily BHB (Ingvartsen, 2006; LeBlanc, 2010). According to McArt et al. (2015), excessive production of NEFA and BHB in healthy cows is indicative of poor adaptation to NEB and can affect different parameters during lactation, including the immune system, health, and milk production.

A postpartal increase in plasma BHB and whole blood BHB was noted in MLGSH cows in this study (Figure 3A and 3B), indicating a higher level of partial oxidation of fatty acids. This observation in MLGSH cows was accompanied by comparable milk production to HGSH cows (44.7 vs. 46.7 kg/d, respectively) but lower glucose (64.9 vs. 69.2 mg/dL, respectively). This corroborates that the heightened BHB produced was necessary to provide energy to peripheral tissues while channeling the available glucose to the mammary gland. This effect was partially supported by a numerically higher genetic potential in MLGSH cows (Supplemental Figure S1), which was potentially crippled by the numerically lower DMI (~2 kg) postpartum when compared with HGSH cows. The postcalving peak of BHB in MLGSH cows was detected by 2 different measurement methods (e.g., whole blood and plasma), highlighting the reliability of this observation. Supporting this effect, we observed a higher incidence of cows diagnosed with ketosis (~66%) in the MLGSH group (Table 2). Lower liver GSH in MLGSH cows could have directly or indirectly predisposed these cows to ketogenesis. Perhaps thiols and disulfide forms of GSH may be necessary to activate or inhibit enzymes related to ketogenesis. For instance, the microsome 3-hydroxy-3-methylglutaryl CoA (**HMG-CoA**) reductase (HMGR), a key enzyme in cholesterol biosynthesis, can be reversibly activated or inhibited by thiols or disulfide forms of GSH, respectively (Cappel and Gilbert, 1988). Similarly, mitochondrial HMG-CoA synthase (encoded by *HMGCS2*), the rate-limiting step in

ketogenesis, contains a critical Cys residue. Oxidation of this residue during acetaminophen-induced GSH depletion can diminish the enzyme's activity (Andringa et al., 2008). Although these findings might imply that reduced liver GSH levels would lead to decreased ketogenesis, extrapolating data from rodent models to transition dairy cows poses challenges. Nevertheless, these observations offer potential insights into how GSH may modulate liver metabolism, underscoring the need for further investigation in this area.

During the acute phase response, the secretion of negative acute-phase proteins (**APP**) and liver function indicators such as albumin and cholesterol decreases, whereas positive APP, such as haptoglobin and ceruloplasmin, are secreted at higher rates. These APP have previously been used to classify liver function in dairy cows (Bertoni and Trevisi, 2013). Cholesterol is synthesized in the liver, with concentrations typically decreasing to nadir levels during the first week of lactation and rapidly increasing afterward. This rise in cholesterol levels in HGSH cows compared with all other groups toward the end of the transition period may indicate recovery in hepatic function (Trevisi et al., 2012), particularly in lipoprotein exportation (LeBlanc et al., 2004). This effect was partially confirmed by the positive correlation between prepartal liver GSH and blood cholesterol at −10 DIM (Table 6) and prepartal liver GSH and mean postpartal cholesterol from 2 to 21 DIM (Supplemental Table S4).

Oxidative stress is caused by the imbalance between the increase of oxidative factors, such as ROM, and depleted antioxidants (Sordillo and Aitken, 2009). Traditionally, oxidative stress has been considered to contribute to inflammatory and immune dysfunction, and, consequently, increased susceptibility to diseases during the transition period (Sordillo and Aitken, 2009). However, more recently, oxidative stress etiology has been attributed to the presence of clinical and subclinical diseases during inflammation (Trevisi and Minuti, 2018). Antioxidants are compounds and molecular systems that can neutralize ROM and can be categorized into enzymatic (e.g., GPx) and nonenzymatic (e.g., GSH and SHp; Bernabucci et al., 2005).

The GPx reduces phospholipid hydroperoxides or lipid peroxidation within cell membranes. In dairy cows, research has primarily focused on the GPx antioxidant system (Sordillo and Aitken, 2009), and there is substantial evidence supporting the importance of selenium (Se) for GPx activity. Although GSH is a clear substrate for GPx activity, we did not observe any associations between prepartal liver GSH and GPx activity in blood, liver, and gene expression. This could be related to a lack of differences in ROM across GSH groups, thereby diminishing the requirement for changes in GPx activity. Alternatively, it is plausible that GPx achieves a saturation point at a specific GSH concentration, beyond which further increases in GSH do not yield a corresponding enhancement in GPx activity. However, information on the specific GSH concentration at which GPx could be potentially saturated has not been well characterized (Vašková et al., 2023).

Thiol groups, which consist of sulfur and hydrogen, represent the sulfhydryl groups of GSH, albumin, Cys, and homocysteine in plasma, of which GSH is the most abundant (Barron, 1951; Bernabucci et al., 2005). These groups are essential for maintaining the redox balance within cells and plasma. In this context, the linear increase in SHp levels across the GSH groups could be attributed to increased prepartal hepatic GSH storage that is released into the bloodstream after calving. These findings align with Bernabucci et al. (2005), who proposed that elevated plasma SH levels around calving may reflect a counterbalance response to neutralize ROM during this critical period. Furthermore, plasma SH levels can provide a reliable estimate of intracellular GSH, highlighting their importance in assessing oxidative balance (van den Berg et al., 1992).

To evaluate the efficacy of antioxidants in mitigating oxidative damage in plasma, we used the FRAP assay. This method quantifies antioxidant capacity by measuring the reduction of ferric ions (Fe^{3+}) to ferrous ions (Fe^{2+}) under acidic conditions (Benzie and Strain, 1996). Our findings revealed no significant differences in FRAP across GSH groups. This observation may be attributed to the limitations of the FRAP assay, as it primarily measures iron-reducing agents rather than sulfhydryl-containing compounds (Prior et al., 2005) and may not adequately reflect the activity of GPx or SHp. Alternative methods, such as the oxygen radical absorbance capacity assay, which quantifies hydrosoluble antioxidants (e.g., albumin) against reactive oxygen species (Mezzetti and Trevisi, 2023), or the measurement of malondialdehyde, a byproduct of lipid peroxidation, may provide more effective indicators of antioxidant capacity and oxidative stress.

During exposure to oxidative stress, reduced GSH is oxidized to GSSG by GPx, and GSSG is then reduced to GSH by GSH reductase, a process that consumes NADPH as a reducing agent and forms the GSH redox cycle (Lu, 2009). Under normal conditions, reduced GSH constitutes ~98% of the total GSH (Lu, 2013). However, during excessive ROM generation, mainly in early lactation, GSH is rapidly oxidized to GSSG, which is then exported out of hepatocytes. This mechanism prevents intracellular GSSG accumulation and ensures redox balance, but it may lead to a depletion of hepatic GSH stores under sustained oxidative stress (Lu, 2009). Therefore, the balance between GSH synthesis and degradation seems to be critical for maintaining GSH storage. A negative correlation was observed between liver GSH and day

relative to calving (Supplemental Figure S2), translating to a decrease in liver GSH as cows approach calving. This decline may result from a reduced availability of GSH constituent AA due to a common decline in DMI in the days leading to calving, coupled with increased AA requirements for fetal development (Bell, 1995) or an increased GSH oxidation rate driven by increasing oxidative stress during this period. However, our results revealed no differences in ROM among GSH groups at −8 DIM (Table 4), which suggests a more complex relationship between oxidative stress and GSH metabolism as cows approach calving. For instance, the lack of hepatic GGT activity across GSH groups at −8 DIM suggests that prepartal liver GSH is less likely to be affected by degradation. Although this remains uncertain, it implies that mechanisms regulating GSH storage may involve factors beyond oxidative stress levels, such as nutrient availability or enzyme activity.

Glutathione Metabolism Gene Expression

To further understand the regulation of GSH metabolism, we analyzed the expression of key genes encoding enzymes involved in GSH synthesis and degradation. The synthesis of GSH particularly occurs through 2 enzymes, glutamate-cysteine ligase (GCL) and GSH synthetase (GSS; Wu et al., 2004). The GCL is composed of 2 subunits: the catalytic subunit (GCLC) and the modifier subunit (GCLM; Lu, 2013). The GCLC subunit contains all the catalytic activity of the enzyme, whereas the GCLM subunit is enzymatically inactive and does not directly catalyze the reaction. The second step is catalyzed by GSS, which produces GSH by adding a Gly molecule to γ-glutamyl-cysteine (Lu, 2013). GCL has been reported as the rate-limiting step in GSH biosynthesis (Dalton et al., 2004). This was supported by findings that overexpression of *GCLC* and not *GSS* is associated with increased GSH levels (Lu, 2013). In addition to GSH biosynthesis, another mechanism to increase the intracellular GSH pool is reducing the GSSG, which is carried out by GSR utilizing NADPH as a cofactor. This plays an important role in maintaining intracellular GSH homeostasis (Lu, 2009). Interestingly, NADPH is generated through the reduction of NADP by glucose-6-phosphate dehydrogenase (encoded by *G6PD*). In the current study, a positive quadratic effect on *G6PD* mRNA expression was observed across the GSH groups (Table 7); however, this effect was not reflected in hepatic reduced GSH at −8 DIM (Figure 4C). This inconsistency could be related to a posttranscriptional regulation of *G6PD* or blood glucose levels following a linear rather than a quadratic increase (Table 5).

In dairy cows, Zhou et al. (2017) observed no effect on *GCLC* and *GSR* expression when transition cows were supplemented with Met, an upstream precursor of Cys through the transulfuration pathway. Similarly Osorio et al. (2014a) did not observe an effect on prepartal liver *GCLC* and *GSR* expression in cows supplemented with Met compared with control. In contrast, Zhou et al. (2018) observed an upregulation of *GCLC* and *GSR* when primary liver cells isolated from dairy cows were incubated with 40 μ*M* Met for 24 h. This suggests that additional metabolic or genetic control points for *GCLC* and *GSR* mRNA expression may exist at the whole animal level in addition to the supply of Cys precursors. Although our study did not involve AA supplementation, we observed a similar upregulation of *GCLC* and *GSR* in cows with elevated liver GSH levels. Although this may partially explain the increments in prepartal liver GSH, it does not provide an explanation for the upregulation of these genes. Although *GCLC* and *GSR* are known target genes of *NFE2L2*, the positive quadratic effect observed in *NFE2L2* was not translated into quadratic effects on *GCLC* and *GSR*. This suggests that *NFE2L2* may have less control over transcriptional regulation of antioxidants during the prepartum period, when cows are less prone to oxidative stress. This gene regulation may be under genetic control; for instance, single nucleotide polymorphisms have been detected in *GCLC* and *GCLM* in humans, which in turn results in a protective effect against type 2 diabetes mediated by increased levels of GSH and decreased oxidative stress (Azarova et al., 2020).

In the glutathione cycle, degradation of extracellular GSH and GSSG is primarily initiated by GGT (Bachhawat and Yadav, 2018). The gamma-glutamyl cyclotransferase (GGCT), previously considered an essential step in the γ-glutamyl cycle (Meister and Tate, 1976), is now considered a peripheral enzyme to the glutathione cycle (Bachhawat and Yadav, 2018). This mammalian-specific enzyme converts γ-glutamyl AA into 5-oxoproline while releasing the AA. Both enzymes (i.e., GGT and GGCT) have a role in maintaining GSH homeostasis by facilitating the recycling of Cys (Bachhawat and Kaur, 2017; He et al., 2021). The observed upregulation of GSH-related enzymes suggests a potential molecular mechanism that increases GSH metabolism and turnover, potentially supporting antioxidant capacity during oxidative stress, sourcing for AA synthesis, and promoting metabolic adaptation during late gestation.

CONCLUSIONS

Our study provides novel insights into the role of liver glutathione in transition dairy cows, highlighting its correlation with lactation performance while promoting metabolic resilience. In particular, the linear increase in ECM and milk protein yield as cows stored greater amounts

of liver GSH before calving underscores the potential of developing nutritional strategies targeting GSH synthesis during late gestation. Cows with greater prepartal liver GSH exhibited greater prepartal EB coupled with greater BCS around the transition period, suggesting a potential link between hepatic GSH reserves and nutrient partitioning during late gestation. The linear upregulation of key GSH metabolism genes (e.g., *GCLC*, *GGT*, *GSR*, and *GGCT*) suggests that transcriptional regulation may contribute to the liver GSH phenotype observed in this study. These results emphasize the importance of maintaining adequate hepatic GSH reserves before calving to support metabolic adaptation and lactation performance.

NOTES

This project was mainly funded by USDA-National Institute of Food and Agriculture (NIFA, Washington, DC, grant #2022-67015-37085). The authors thank the staff at the Virginia Tech Dairy Complex for their help with the animal study. Supplemental material for this article is available at https://hdl.handle.net/10919/137794. All procedures were conducted under protocols approved by the Virginia Tech Institutional Animal Care and Use Committee (protocol no. 22-071). The authors have not stated any conflicts of interest.

Nonstandard abbreviations used: APP = acute-phase protein; EB = energy balance; FRAP = ferric reducing antioxidant power; G × T = group × time interaction; GCL = L-glutamate L-cysteine γ-ligase; GGT = gamma-glutamyl-transferase; GOT = glutamic-oxaloacetic transaminase; GPx = GSH peroxidase; GSH = glutathione; GSS = GSH synthetase; GSSG = oxidized GSH; HGSH = high GSH; HMG-CoA = 3-hydroxy-3-methylglutaryl CoA; LGSH = low GSH; MHGSH = medium-high GSH; MLGSH = medium-low GSH; MPO = myeloperoxidase; NEB = negative energy balance; NEFA = nonesterified fatty acid; NEI = net energy intake; NE_{Milk} = NEL for milk production; NEP = NEL for gestation; qPCR = quantitative PCR; RBC = red blood cell; RFU = relative fluorescence unit; ROM = reactive oxygen metabolite; RPM = rumen-protected methionine; SHp = total thiol groups of plasma; TAG = triacylglyceride.

REFERENCES

Abuelo, A., J. Hernandez, J. L. Benedito, and C. Castillo. 2015. The importance of the oxidative status of dairy cattle in the periparturient period: Revisiting antioxidant supplementation. J. Anim. Physiol. Anim. Nutr. (Berl.) 99:1003–1016. https://doi.org/10.1111/jpn.12273.

Andringa, K. K., M. L. Bajt, H. Jaeschke, and S. M. Bailey. 2008. Mitochondrial protein thiol modifications in acetaminophen hepatotoxicity: Effect on HMG-CoA synthase. Toxicol. Lett. 177:188–197. https://doi.org/10.1016/j.toxlet.2008.01.010.

AOAC International. 2000. Official Methods of Analysis of AOAC International. 17th ed. AOAC International, Gaithersburg, MD.

AOAC International. 2006. Official Methods of Analysis of AOAC International. 18th ed. AOAC International, Gaithersburg, MD.

Atroshi, F., and M. Sandholm. 1982. Red blood cell glutathione as a marker of milk production in Finn sheep. Res. Vet. Sci. 33:256–259. https://doi.org/10.1016/S0034-5288(18)32346-4.

Azarova, I., E. Klyosova, V. Lazarenko, A. Konoplya, and A. Polonikov. 2020. Genetic variants in glutamate cysteine ligase confer protection against type 2 diabetes. Mol. Biol. Rep. 47:5793–5805. https://doi.org/10.1007/s11033-020-05647-5.

Bachhawat, A. K., and A. Kaur. 2017. Glutathione degradation. Antioxid. Redox Signal. 27:1200–1216. https://doi.org/10.1089/ars.2017.7136.

Bachhawat, A. K., and S. Yadav. 2018. The glutathione cycle: Glutathione metabolism beyond the gamma-glutamyl cycle. IUBMB Life 70:585–592. https://doi.org/10.1002/iub.1756.

Barron, E. S. 1951. Thiol groups of biological importance. Adv. Enzymol. Relat. Subj. Biochem. 11:201–266.

Batistel, F., J. M. Arroyo, C. I. M. Garces, E. Trevisi, C. Parys, M. A. Ballou, F. C. Cardoso, and J. J. Loor. 2018. Ethyl-cellulose rumen-protected methionine alleviates inflammation and oxidative stress and improves neutrophil function during the periparturient period and early lactation in Holstein dairy cows. J. Dairy Sci. 101:480–490. https://doi.org/10.3168/jds.2017-13185.

Bauman, D. E., and W. B. Currie. 1980. Partitioning of nutrients during pregnancy and lactation: a review of mechanisms involving homeostasis and homeorhesis. J. Dairy Sci. 63:1514–1529. https://doi.org/10.3168/jds.S0022-0302(80)83111-0.

Baumgard, L. H., R. J. Collier, and D. E. Bauman. 2017. A 100-Year Review: Regulation of nutrient partitioning to support lactation. J. Dairy Sci. 100:10353–10366. https://doi.org/10.3168/jds.2017-13242.

Baumrucker, C. R. 1985. Amino acid transport systems in bovine mammary tissue. J. Dairy Sci. 68:2436–2451. https://doi.org/10.3168/jds.S0022-0302(85)81119-X.

Baumrucker, C. R., and P. A. Pocius. 1978. γ-Glutamyl transpeptidase in lactating mammary secretory tissue of cow and rat. J. Dairy Sci. 61:309–314. https://doi.org/10.3168/jds.S0022-0302(78)83599-1.

Bell, A. W. 1995. Regulation of organic nutrient metabolism during transition from late pregnancy to early lactation. J. Anim. Sci. 73:2804–2819. https://doi.org/10.2527/1995.7392804x.

Benzie, I. F., and J. J. Strain. 1996. The ferric reducing ability of plasma (FRAP) as a measure of "antioxidant power": The FRAP assay. Anal. Biochem. 239:70–76. https://doi.org/10.1006/abio.1996.0292.

Bernabucci, U., B. Ronchi, N. Lacetera, and A. Nardone. 2005. Influence of body condition score on relationships between metabolic status and oxidative stress in periparturient dairy cows. J. Dairy Sci. 88:2017–2026. https://doi.org/10.3168/jds.S0022-0302(05)72878-2.

Bertoni, G., and E. Trevisi. 2013. Use of the liver activity index and other metabolic variables in the assessment of metabolic health in dairy herds. Vet. Clin. North Am. Food Anim. Pract. 29:413–431. https://doi.org/10.1016/j.cvfa.2013.04.004.

Bionaz, M., and J. J. Loor. 2007. Identification of reference genes for quantitative real-time PCR in the bovine mammary gland during the lactation cycle. Physiol. Genomics 29:312–319. https://doi.org/10.1152/physiolgenomics.00223.2006.

Bucktrout, R. E., N. Ma, A. Aboragah, A. S. Alharthi, Y. Liang, V. Lopreiato, M. G. Lopes, E. Trevisi, I. A. Alhidary, C. Fernandez, and J. J. Loor. 2021. One-carbon, carnitine, and glutathione metabolism-related biomarkers in peripartal Holstein cows are altered by prepartal body condition. J. Dairy Sci. 104:3403–3417. https://doi.org/10.3168/jds.2020-19402.

Cappel, R. E., and H. F. Gilbert. 1988. Thiol/disulfide exchange between 3-hydroxy-3-methylglutaryl-CoA reductase and glutathione. A thermodynamically facile dithiol oxidation. J. Biol. Chem. 263:12204–12212. https://doi.org/10.1016/S0021-9258(18)37740-8.

Coleman, D. N., A. S. Alharthi, Y. Liang, M. G. Lopes, V. Lopreiato, M. Vailati-Riboni, and J. J. Loor. 2021. Multifaceted role of one-carbon metabolism on immunometabolic control and growth during preg-

nancy, lactation and the neonatal period in dairy cattle. J. Anim. Sci. Biotechnol. 12:27. https://doi.org/10.1186/s40104-021-00547-5.

Dalton, T. P., Y. Chen, S. N. Schneider, D. W. Nebert, and H. G. Shertzer. 2004. Genetically altered mice to evaluate glutathione homeostasis in health and disease. Free Radic. Biol. Med. 37:1511–1526. https://doi.org/10.1016/j.freeradbiomed.2004.06.040.

Drackley, J. K. 1999. ADSA Foundation Scholar Award: Biology of dairy cows during the transition period: The final frontier? J. Dairy Sci. 82:2259–2273. https://doi.org/10.3168/jds.S0022-0302(99)75474-3.

Goering, H. K., and P. J. Van Soest. 1970. Forage Fiber Analyses (Apparatus, Reagents, Procedures, and Some Applications). USDA Agricultural Research Service, Washington, DC.

Grummer, R. R. 1995. Impact of changes in organic nutrient metabolism on feeding the transition dairy cow. J. Anim. Sci. 73:2820–2833. https://doi.org/10.2527/1995.7392820x.

Hall, M. B. 2009. Determination of starch, including maltooligosaccharides, in animal feeds: comparison of methods and a method recommended for AOAC collaborative study. J. AOAC Int. 92:42–49. https://doi.org/10.1093/jaoac/92.1.42.

Hall, M. B. 2023. *Invited review:* Corrected milk: Reconsideration of common equations and milk energy estimates. J. Dairy Sci. 106:2230–2246. https://doi.org/10.3168/jds.2022-22219.

He, Z., X. Sun, S. Wang, D. Bai, X. Zhao, Y. Han, P. Hao, and X. S. Liu. 2021. Ggct (gamma-glutamyl cyclotransferase) plays an important role in erythrocyte antioxidant defense and red blood cell survival. Br. J. Haematol. 195:267–275. https://doi.org/10.1111/bjh.17775.

Ingvartsen, K. L. 2006. Feeding-and management-related diseases in the transition cow: Physiological adaptations around calving and strategies to reduce feeding-related diseases. Anim. Feed Sci. Technol. 126:175–213. https://doi.org/10.1016/j.anifeedsci.2005.08.003.

Johnston, S. L., K. E. Kitson, J. W. Tweedie, S. R. Davis, and J. Lee. 2004. γ-Glutamyl transpeptidase inhibition suppresses milk protein synthesis in isolated ovine mammary cells. J. Dairy Sci. 87:321–329. https://doi.org/10.3168/jds.S0022-0302(04)73171-9.

Larsen, M., and N. B. Kristensen. 2013. Precursors for liver gluconeogenesis in periparturient dairy cows. Animal 7:1640–1650. https://doi.org/10.1017/S1751731113001171.

LeBlanc, S. 2010. Monitoring metabolic health of dairy cattle in the transition period. J. Reprod. Dev. 56(Suppl.):S29–S35. https://doi.org/10.1262/jrd.1056S29.

LeBlanc, S. J., T. H. Herdt, W. M. Seymour, T. F. Duffield, and K. E. Leslie. 2004. Peripartum serum vitamin E, retinol, and beta-carotene in dairy cattle and their associations with disease. J. Dairy Sci. 87:609–619. https://doi.org/10.3168/jds.S0022-0302(04)73203-8.

Lu, S. C. 2009. Regulation of glutathione synthesis. Mol. Aspects Med. 30:42–59. https://doi.org/10.1016/j.mam.2008.05.005.

Lu, S. C. 2013. Glutathione synthesis. Biochim. Biophys. Acta, Gen. Subj. 1830:3143–3153. https://doi.org/10.1016/j.bbagen.2012.09.008.

McArt, J. A., D. V. Nydam, and M. W. Overton. 2015. Hyperketonemia in early lactation dairy cattle: A deterministic estimate of component and total cost per case. J. Dairy Sci. 98:2043–2054. https://doi.org/10.3168/jds.2014-8740.

Meister, A., and S. S. Tate. 1976. Glutathione and related gamma-glutamyl compounds: biosynthesis and utilization. Annu. Rev. Biochem. 45:559–604. https://doi.org/10.1146/annurev.bi.45.070176.003015.

Mezzetti, M., A. Minuti, F. Piccioli-Cappelli, M. Amadori, M. Bionaz, and E. Trevisi. 2019. The role of altered immune function during the dry period in promoting the development of subclinical ketosis in early lactation. J. Dairy Sci. 102:9241–9258. https://doi.org/10.3168/jds.2019-16497.

Mezzetti, M., and E. Trevisi. 2023. Methods of Evaluating the Potential Success or Failure of Transition Dairy Cows. Vet. Clin. North Am. Food Anim. Pract. 39:219–239. https://doi.org/10.1016/j.cvfa.2023.02.008.

NASEM (National Academies of Sciences, Engineering, and Medicine). 2021. Nutrient Requirements of Dairy Cattle: 8th rev. ed. The National Academies Press, Washington, DC.

Osorio, J. S., P. Ji, J. K. Drackley, D. Luchini, and J. J. Loor. 2014a. Smartamine M and MetaSmart supplementation during the peripartal period alter hepatic expression of gene networks in 1-carbon metabolism, inflammation, oxidative stress, and the growth hormone-insulin-like growth factor 1 axis pathways. J. Dairy Sci. 97:7451–7464. https://doi.org/10.3168/jds.2014-8680.

Osorio, J. S., E. Trevisi, P. Ji, J. K. Drackley, D. Luchini, G. Bertoni, and J. J. Loor. 2014b. Biomarkers of inflammation, metabolism, and oxidative stress in blood, liver, and milk reveal a better immunometabolic status in peripartal cows supplemented with Smartamine M or MetaSmart. J. Dairy Sci. 97:7437–7450. https://doi.org/10.3168/jds.2013-7679.

Pero, M. E., N. Mirabella, P. Lombardi, C. Squillacioti, A. De Luca, and L. Avallone. 2006. Gammaglutamyltransferase activity in buffalo mammary tissue during lactation. Anim. Sci. 82:351–354. https://doi.org/10.1079/ASC200635.

Pocius, P. A., J. H. Clark, and C. R. Baumrucker. 1981. Glutathione in bovine blood: possible source of amino acids for milk protein synthesis. J. Dairy Sci. 64:1551–1554. https://doi.org/10.3168/jds.S0022-0302(81)82724-5.

Prior, R. L., X. Wu, and K. Schaich. 2005. Standardized methods for the determination of antioxidant capacity and phenolics in foods and dietary supplements. J. Agric. Food Chem. 53:4290–4302. https://doi.org/10.1021/jf0502698.

Rosa, F., T. C. Michelotti, B. St-Pierre, E. Trevisi, and J. S. Osorio. 2021. Early life fecal microbiota transplantation in neonatal dairy calves promotes growth performance and alleviates inflammation and oxidative stress during weaning. Animals (Basel) 11:2704.

Sáez, G. T., F. J. Romero, and J. Vina. 1985. Effects of glutathione depletion on gluconeogenesis in isolated hepatocytes. Arch. Biochem. Biophys. 241:75–80. https://doi.org/10.1016/0003-9861(85)90363-7.

Sordillo, L. M. 2016. Nutritional strategies to optimize dairy cattle immunity. J. Dairy Sci. 99:4967–4982. https://doi.org/10.3168/jds.2015-10354.

Sordillo, L. M., and S. L. Aitken. 2009. Impact of oxidative stress on the health and immune function of dairy cattle. Vet. Immunol. Immunopathol. 128:104–109. https://doi.org/10.1016/j.vetimm.2008.10.305.

Trevisi, E., M. Amadori, S. Cogrossi, E. Razzuoli, and G. Bertoni. 2012. Metabolic stress and inflammatory response in high-yielding, periparturient dairy cows. Res. Vet. Sci. 93:695–704. https://doi.org/10.1016/j.rvsc.2011.11.008.

Trevisi, E., and A. Minuti. 2018. Assessment of the innate immune response in the periparturient cow. Res. Vet. Sci. 116:47–54. https://doi.org/10.1016/j.rvsc.2017.12.001.

van den Berg, J. J., J. A. Op den Kamp, B. H. Lubin, B. Roelofsen, and F. A. Kuypers. 1992. Kinetics and site specificity of hydroperoxide-induced oxidative damage in red blood cells. Free Radic. Biol. Med. 12:487–498. https://doi.org/10.1016/0891-5849(92)90102-M.

Van Soest, P. J., J. B. Robertson, and B. A. Lewis. 1991. Methods for dietary fiber, neutral detergent fiber, and nonstarch polysaccharides in relation to animal nutrition. J. Dairy Sci. 74:3583–3597. https://doi.org/10.3168/jds.S0022-0302(91)78551-2.

Vašková, J., L. Kocan, L. Vasko, and P. Perjesi. 2023. Glutathione-related enzymes and proteins: A review. Molecules 28:1447. https://doi.org/10.3390/molecules28031447.

Vázquez-Meza, H., M. M. Vilchis-Landeros, M. Vazquez-Carrada, D. Uribe-Ramirez, and D. Matuz-Mares. 2023. Cellular compartmentalization, glutathione transport and its relevance in some pathologies. Antioxidants 12:834. https://doi.org/10.3390/antiox12040834.

Wu, G., J. R. Lupton, N. D. Turner, Y.-Z. Fang, and S. Yang. 2004. Glutathione metabolism and its implications for health. J. Nutr. 134:489–492. https://doi.org/10.1093/jn/134.3.489.

Yoder, P. S., X. Huang, I. A. Teixeira, J. P. Cant, and M. D. Hanigan. 2020. Effects of jugular infused methionine, lysine, and histidine as a group or leucine and isoleucine as a group on production and metabolism in lactating dairy cows. J. Dairy Sci. 103:2387–2404. https://doi.org/10.3168/jds.2019-17082.

Zhou, Y. F., Z. Zhou, F. Batistel, I. Martinez-Cortes, R. T. Pate, D. L. Luchini, and J. J. Loor. 2018. Methionine and choline supply alter transmethylation, transsulfuration, and cytidine 5′-diphosphocholine pathways to different extents in isolated primary liver cells from dairy cows. J. Dairy Sci. 101:11384–11395. https://doi.org/10.3168/jds.2017-14236.

Zhou, Z., O. Bulgari, M. Vailati-Riboni, E. Trevisi, M. A. Ballou, F. C. Cardoso, D. N. Luchini, and J. J. Loor. 2016. Rumen-protected methionine compared with rumen-protected choline improves immunometabolic status in dairy cows during the peripartal period. J. Dairy Sci. 99:8956–8969. https://doi.org/10.3168/jds.2016-10986.

Zhou, Z., T. A. Garrow, X. Dong, D. N. Luchini, and J. J. Loor. 2017. Hepatic activity and transcription of betaine-homocysteine methyltransferase, methionine synthase, and cystathionine synthase in periparturient dairy cows are altered to different extents by supply of methionine and choline. J. Nutr. 147:11–19. https://doi.org/10.3945/jn.116.240234.